

Contact mechanics and elements of tribology

Lecture 4. *Micromechanical contact: roughness*

Vladislav A. Yastrebov

*Mines Paris - PSL, CNRS
Centre des Matériaux, Evry, France*



@ Centre des Matériaux (& virtually)
February 25, 2025



Creative Commons BY
Vladislav A. Yastrebov

- Introduction
- Measurement techniques
- Classifications
- Main characteristics
- PDF and PSD
- Random process model of roughness
- Computational roughness models
- Reading

Contact under microscope

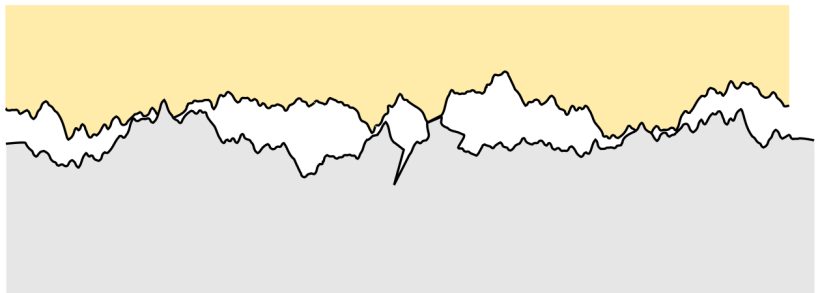


traceygear.com

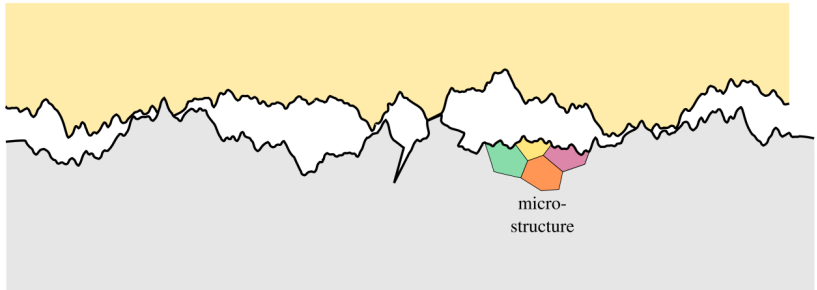
Contact under microscope



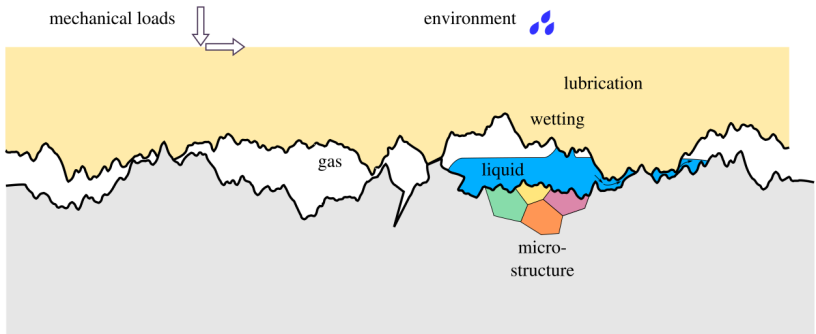
Contact under microscope



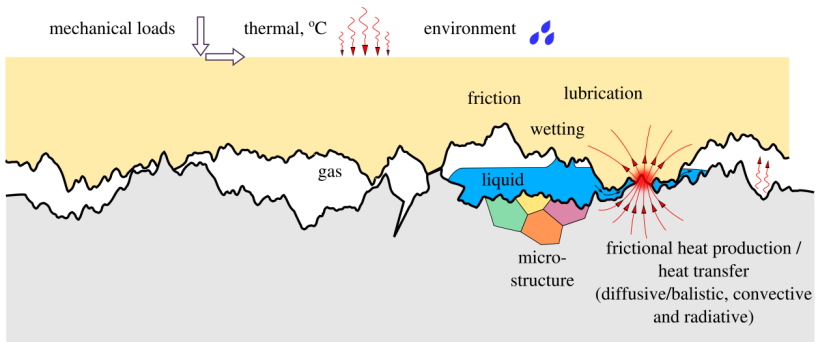
Contact under microscope



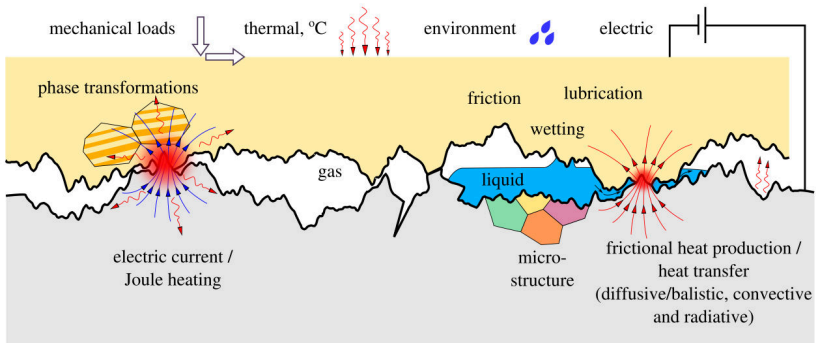
Contact under microscope



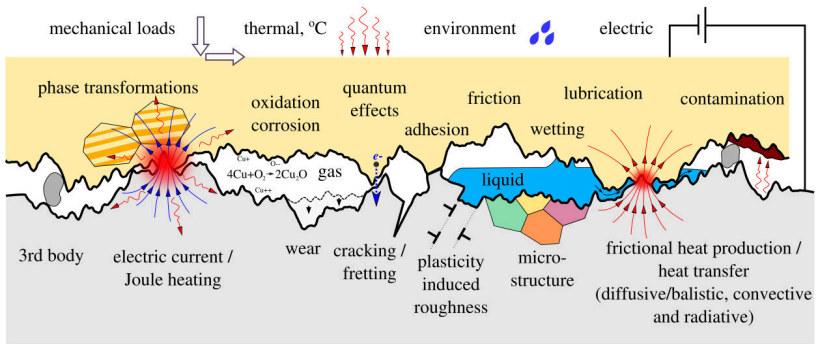
Contact under microscope



Contact under microscope



Contact under microscope



Roughness

- Natural and industrial surfaces are *rough*:

- processing
- polishing
- coating
- microstructure
- surface energy
- deformation
- aging
- environment

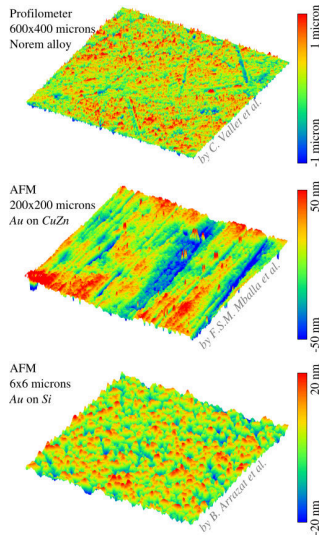


Fig. Examples of rough surfaces

Roughness

- Natural and industrial surfaces are *rough*:

- processing
- polishing
- coating
- microstructure
- surface energy
- deformation
- aging
- environment

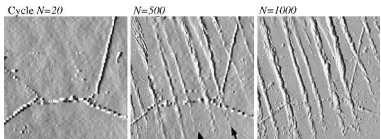


Fig. Persistent slip marks [1]

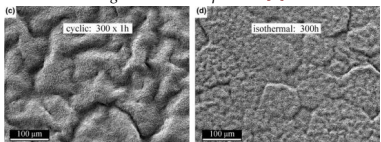


Fig. Rumpling (thermal cycling induced roughness in air)[2]

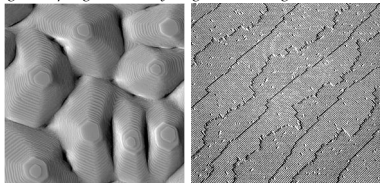


Fig. Epitaxial surface growth [3,4]

[1] J. Polák, J. Man & K. Orbtík, Int J Fatigue 25 (2003)

[2] V.K. Tolpygo, D.R. Clarke, Acta Mat 52 (2004)

[3] M. Einax, W. Dieterich, P. Maass, Rev Mod Phys 85 (2013)

[4] J.R. Arthur, Surf Sci 500 (2002)

Roughness

- Natural and industrial surfaces are *rough*:

- processing
- polishing
- coating
- microstructure
- surface energy
- deformation
- aging
- environment

- Roughness affects:

- stress-strain state
- dry friction
- wear
- adhesion
- fluid flow
- sealing
- energy transfer

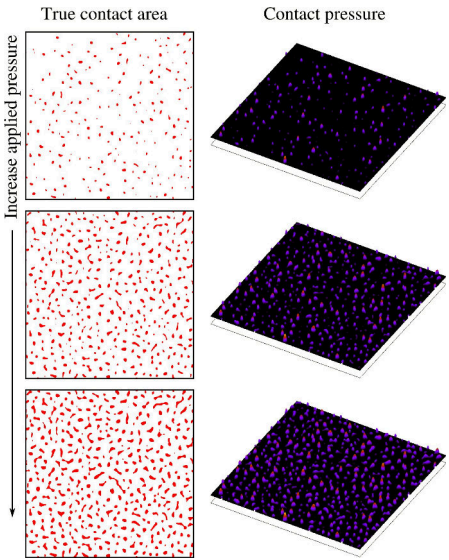


Fig. True contact area and stress fluctuations

Roughness

- Natural and industrial surfaces are *rough*:

- processing
- polishing
- coating
- microstructure
- surface energy
- deformation
- aging
- environment

- Roughness affects:

- stress-strain state
- dry friction
- wear
- adhesion
- fluid flow
- sealing
- energy transfer

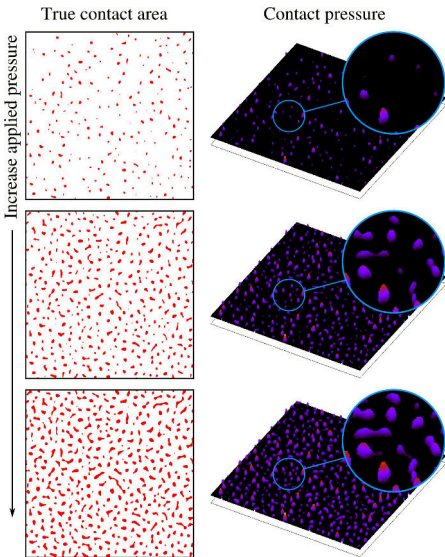


Fig. True contact area and stress fluctuations

Roughness

- Natural and industrial surfaces are *rough*:

- processing
- polishing
- coating
- microstructure
- surface energy
- deformation
- aging
- environment

- Roughness affects:

- stress-strain state
- dry friction
- wear
- adhesion
- fluid flow
- sealing
- energy transfer

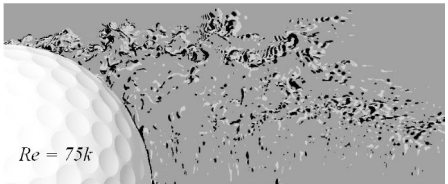
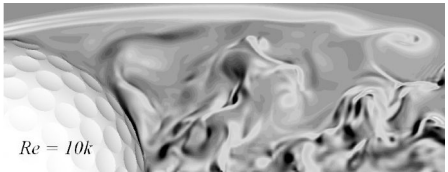


Fig. Numerical simulation of airflow around a (dimpled) golf ball [5]

Roughness

- Natural and industrial surfaces are *rough*:

- processing
- polishing
- coating
- microstructure
- surface energy
- deformation
- aging
- environment

- Roughness affects:

- stress-strain state
- dry friction
- wear
- adhesion
- fluid flow
- sealing
- energy transfer

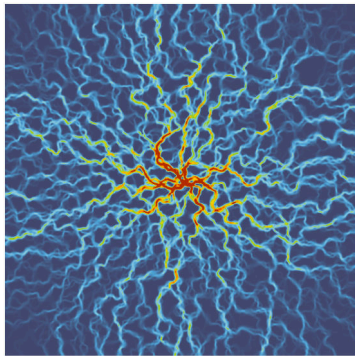


Fig. Fluid passage through free volume between rough surfaces

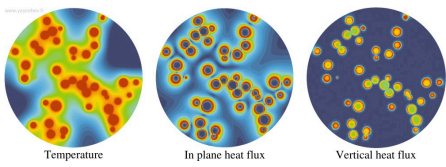
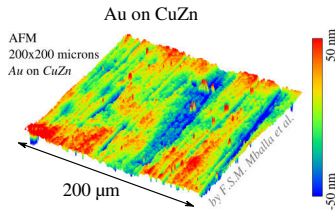
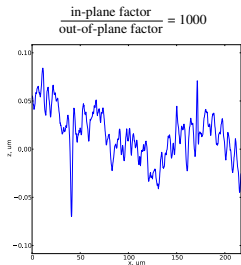
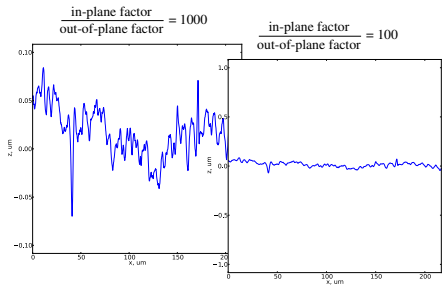


Fig. Heat transfer between rough surfaces
(asperity-based model)

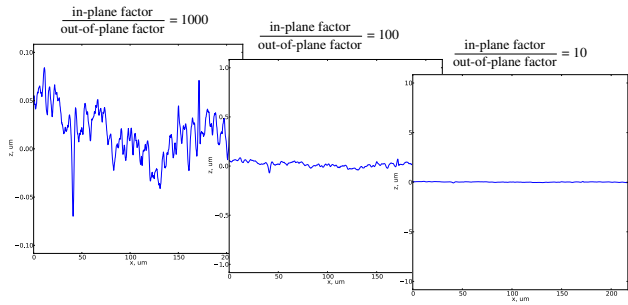
Roughness: in plane and out of plane scales



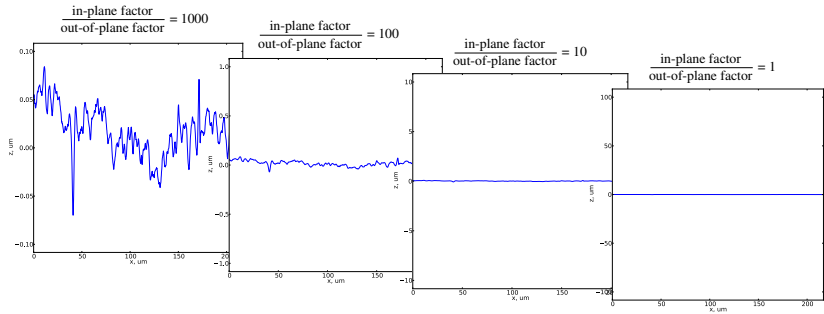
Roughness: in plane and out of plane scales



Roughness: in plane and out of plane scales

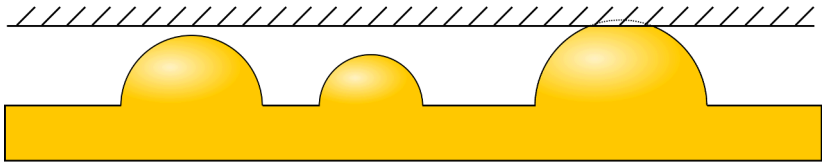


Roughness: in plane and out of plane scales



Roughness: in plane and out of plane scales

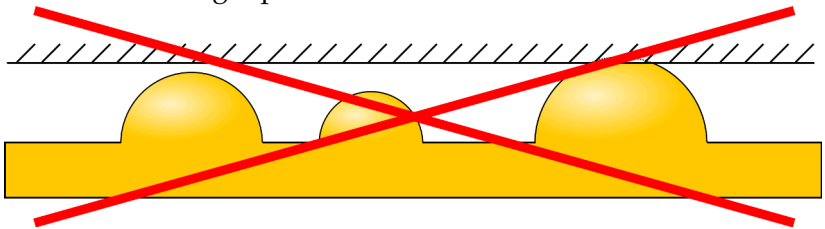
Confusing representation that should be avoided:



Still Hertzian solution remains valid at asperity tips

Roughness: in plane and out of plane scales

Confusing representation that should be avoided:



Still Hertzian solution remains valid at asperity tips

Surface metrology techniques

■ Stylus measurements

- Mechanical contact of a tip with surface
- Force $\geq 3\mu\text{g}$, tip radius $\geq 50\text{ nm}$
- Mainly for profile measurements $y(x)$

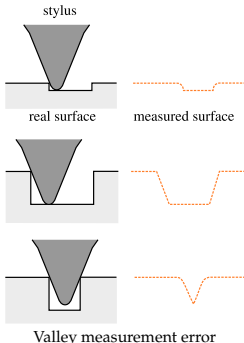
■ Optical measurements

- Confocal (laser scanning) microscopy
- *highest lateral resolution*
- Interferometry (WLI):
- *highest vertical resolution*
- *10 to 100 times faster than CM*
- Scanning Electronic Microscopy (SEM):
- *in secondary electron emission*
- *electrons penetrate in the matter → roughness smoothing*
- *conducting materials*

■ Nano-contact measurements

- Atomic Force Microscopy (AFM)
roughness + adhesive and elastic properties
- Scanning Tunneling Microscope (STM)

Stylus profilometer



Surface metrology techniques

■ Stylus measurements

- Mechanical contact of a tip with surface
- Force $\geq 3\mu\text{g}$, tip radius $\geq 50\text{ nm}$
- Mainly for profile measurements $y(x)$

■ Optical measurements

- Confocal (laser scanning) microscopy
 - *highest lateral resolution*
- Interferometry (WLI):
 - *highest vertical resolution*
 - *10 to 100 times faster than CM*
- Scanning Electronic Microscopy (SEM):
 - *in secondary electron emission*
 - *electrons penetrate in the matter → roughness smoothing*
 - *conducting materials*

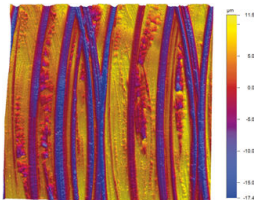
■ Nano-contact measurements

- Atomic Force Microscopy (AFM)
roughness + adhesive and elastic properties
- Scanning Tunneling Microscope (STM)

Stylus profilometer



Modern stylus profilometer
www.bruker.com



Roughness measurements ($\Delta z \approx 30\text{ }\mu\text{m}$)
www.icryst.com

Surface metrology techniques

■ Stylus measurements

- Mechanical contact of a tip with surface
- Force $\geq 3\mu\text{g}$, tip radius $\geq 50\text{ nm}$
- Mainly for profile measurements $y(x)$

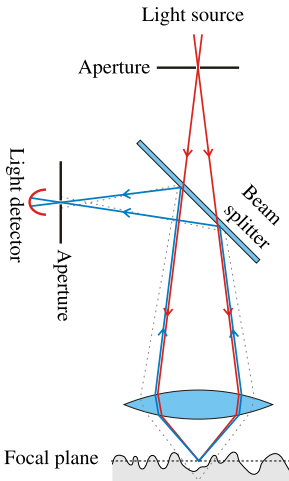
■ Optical measurements

- Confocal (laser scanning) microscopy
- *highest lateral resolution*
- Interferometry (WLI):
- *highest vertical resolution*
- *10 to 100 times faster than CM*
- Scanning Electronic Microscopy (SEM):
- *in secondary electron emission*
- *electrons penetrate in the matter → roughness smoothing*
- *conducting materials*

■ Nano-contact measurements

- Atomic Force Microscopy (AFM)
roughness + adhesive and elastic properties
- Scanning Tunneling Microscope (STM)

Confocal microscopy



Principle of confocal microscopy
adapted from www.wikipedia.org

Surface metrology techniques

■ Stylus measurements

- Mechanical contact of a tip with surface
- Force $\geq 3\mu\text{g}$, tip radius $\geq 50\text{ nm}$
- Mainly for profile measurements $y(x)$

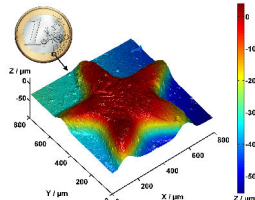
■ Optical measurements

- Confocal (laser scanning) microscopy
- *highest lateral resolution*
- Interferometry (WLI):
- *highest vertical resolution*
- *10 to 100 times faster than CM*
- Scanning Electronic Microscopy (SEM):
- *in secondary electron emission*
- *electrons penetrate in the matter → roughness smoothing*
- *conducting materials*

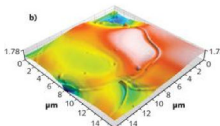
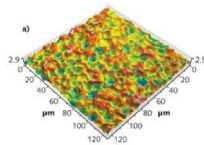
■ Nano-contact measurements

- Atomic Force Microscopy (AFM)
roughness + adhesive and elastic properties Stainless steel machined with micro-electric discharge www.laserfocusworld.org
- Scanning Tunneling Microscope (STM)

Confocal microscopy



1 euro surface www.wikipedia.org



Surface metrology techniques

■ Stylus measurements

- Mechanical contact of a tip with surface
- Force $\geq 3\mu\text{g}$, tip radius $\geq 50\text{ nm}$
- Mainly for profile measurements $y(x)$

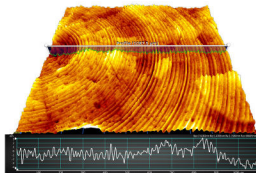
■ Optical measurements

- Confocal (laser scanning) microscopy
- *highest lateral resolution*
- Interferometry (WLI):
- *highest vertical resolution*
- *10 to 100 times faster than CM*
- Scanning Electronic Microscopy (SEM):
- *in secondary electron emission*
- *electrons penetrate in the matter → roughness smoothing*
- *conducting materials*

■ Nano-contact measurements

- Atomic Force Microscopy (AFM)
roughness + adhesive and elastic properties
- Scanning Tunneling Microscope (STM)

White Light Interferometry



Diamond-turned optics www.zygo.com



US quarter surface www.zygo.com

Surface metrology techniques

■ Stylus measurements

- Mechanical contact of a tip with surface
- Force $\geq 3\mu\text{g}$, tip radius $\geq 50 \text{ nm}$
- Mainly for profile measurements $y(x)$

■ Optical measurements

- Confocal (laser scanning) microscopy
 - *highest lateral resolution*
- Interferometry (WLI):
 - *highest vertical resolution*
 - *10 to 100 times faster than CM*
- Scanning Electronic Microscopy (SEM):
 - *in secondary electron emission*
 - *electrons penetrate in the matter → roughness smoothing*
 - *conducting materials*

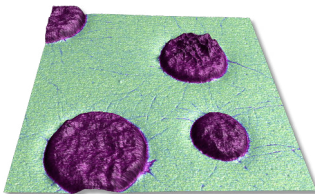
■ Nano-contact measurements

- Atomic Force Microscopy (AFM)
roughness + adhesive and elastic properties
- Scanning Tunneling Microscope (STM)

AFM



Modern AFM
www.bruker.com



Roughness and elastic moduli (color) of polymer blend
www.bruker.com

Surface metrology techniques

■ Stylus measurements

- Mechanical contact of a tip with surface
- Force $\geq 3\mu\text{g}$, tip radius $\geq 50 \text{ nm}$
- Mainly for profile measurements $y(x)$

■ Optical measurements

- Confocal (laser scanning) microscopy
 - *highest lateral resolution*
- Interferometry (WLI):
 - *highest vertical resolution*
 - *10 to 100 times faster than CM*
- Scanning Electronic Microscopy (SEM):
 - *in secondary electron emission*
 - *electrons penetrate in the matter → roughness smoothing*
 - *conducting materials*

■ Nano-contact measurements

- Atomic Force Microscopy (AFM)
roughness + adhesive and elastic properties
- Scanning Tunneling Microscope (STM)

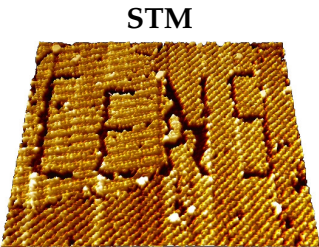
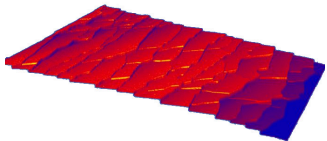


Fig. Center for NanoScience logo
imprinted at atomic scale

www.cens.de



Atomic steps on platinum surface
(500×500 nm)

www.icryst.com

Topography Challenge

"The Surface-Topography Challenge: A Multi-Laboratory Benchmark Study to Advance the Characterization of Topography" just submitted

Roughness: classification

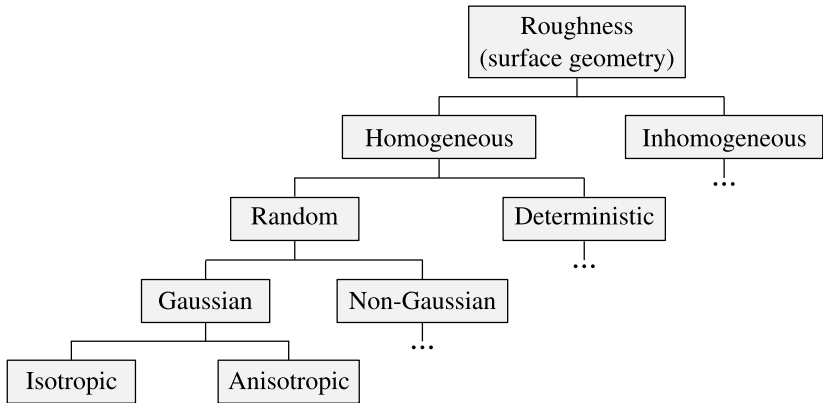


Fig. Roughness classification according to Nayak^[1]

[1] Nayak, J. Lub. Tech. (ASME) 93:398 (1971)

Roughness: classification

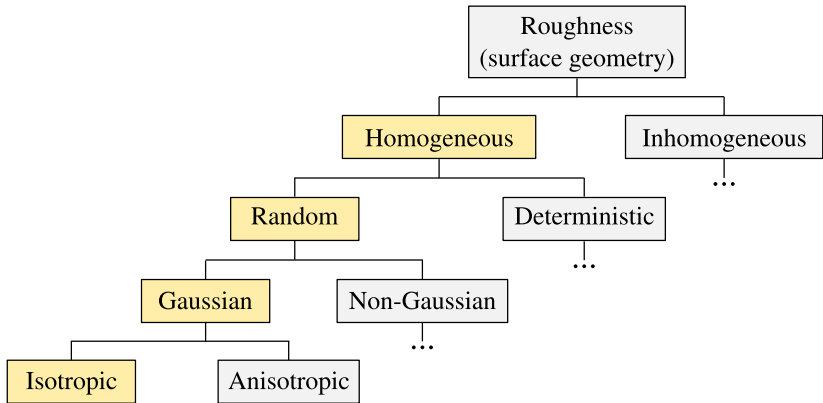


Fig. Roughness classification according to Nayak^[1]

[1] Nayak, J. Lub. Tech. (ASME) 93:398 (1971)

Roughness and geometry/form

- Roughness vs geometry of surfaces
- Sometimes macroscopic geometry is subtracted (filtered out):
form → error of form → waviness → roughness
- Non-trivial to remove macroscopic shape
- Most roughness measurement tools enable shape removal

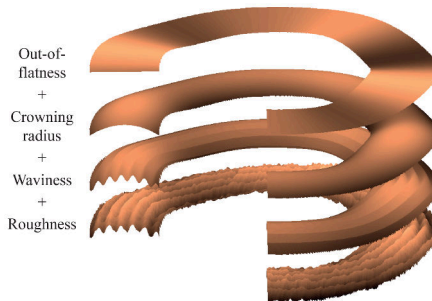


Fig. Circular metallic seal with turned copper surface^[1]

[1] F.P. Rafols, Licentiate Thesis, LTU 2016.

Roughness and geometry/form

- Roughness vs geometry of surfaces
- Sometimes macroscopic geometry is subtracted (filtered out):
form→error of form→waviness→roughness
- Non-trivial to remove macroscopic shape
- Most roughness measurement tools enable shape removal

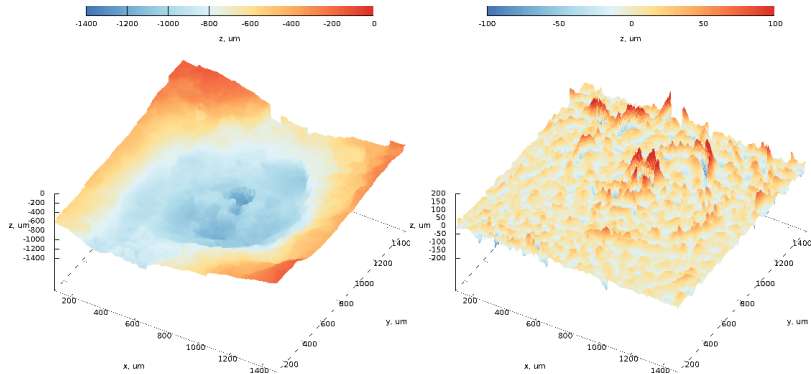


Fig. (left) impact crater, (right) shape is filtered out

Roughness and geometry/form

- Roughness vs geometry of surfaces
- Sometimes macroscopic geometry is subtracted (filtered out):
form → error of form → waviness → roughness
- Non-trivial to remove macroscopic shape
- Most roughness measurement tools enable shape removal

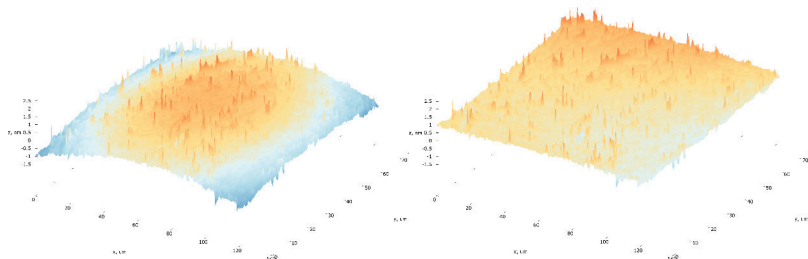


Fig. (left) spherical indenter, (right) $z = a(x^2 + y^2)$ shape is subtracted

Main characteristics

Integral quantities

- Average of absolute values [l.u.] (profile - R_a , surface - S_a)

$$S_a = \frac{1}{A} \int_A |z(x, y) - \bar{z}| dA, \quad S_a = \frac{1}{N^2} \sum_{i=1}^N \sum_{j=1}^N |z_{ij} - \bar{z}|$$

Main characteristics

Integral quantities

- Average of absolute values [l.u.] (profile - R_a , surface - S_a)

$$S_a = \frac{1}{A} \int_A |z(x, y) - \bar{z}| dA, \quad S_a = \frac{1}{N^2} \sum_{i=1}^N \sum_{j=1}^N |z_{ij} - \bar{z}|$$

- Standard deviation of height [l.u.] (σ or R_q for profile, S_q for surface)

$$\sigma = \sqrt{\frac{1}{A} \int_A (z(x, y) - \bar{z})^2 dA}, \quad \sigma = \frac{1}{N} \sqrt{\sum_{i=1}^N \sum_{j=1}^N (z_{ij} - \bar{z})^2}$$

Main characteristics

Integral quantities

- Average of absolute values [l.u.] (profile - R_a , surface - S_a)

$$S_a = \frac{1}{A} \int_A |z(x, y) - \bar{z}| dA, \quad S_a = \frac{1}{N^2} \sum_{i=1}^N \sum_{j=1}^N |z_{ij} - \bar{z}|$$

- Standard deviation of height [l.u.] (σ or R_q for profile, S_q for surface)

$$\sigma = \sqrt{\frac{1}{A} \int_A (z(x, y) - \bar{z})^2 dA}, \quad \sigma = \frac{1}{N} \sqrt{\sum_{i=1}^N \sum_{j=1}^N (z_{ij} - \bar{z})^2}$$

- Maximal valley depth R_v, S_v , maximal peak height R_p, S_p [l.u.]
very sensitive to sample area

Main characteristics

Integral quantities

- Average of absolute values [l.u.] (profile - R_a , surface - S_a)

$$S_a = \frac{1}{A} \int_A |z(x, y) - \bar{z}| dA, \quad S_a = \frac{1}{N^2} \sum_{i=1}^N \sum_{j=1}^N |z_{ij} - \bar{z}|$$

- Standard deviation of height [l.u.] (σ or R_q for profile, S_q for surface)

$$\sigma = \sqrt{\frac{1}{A} \int_A (z(x, y) - \bar{z})^2 dA}, \quad \sigma = \frac{1}{N} \sqrt{\sum_{i=1}^N \sum_{j=1}^N (z_{ij} - \bar{z})^2}$$

- Maximal valley depth R_v, S_v , maximal peak height R_p, S_p [l.u.]
very sensitive to sample area
- Skewness [adim] (γ_1 or R_{sk}, S_{sk})

$$\gamma_1 = \frac{1}{A\sigma^3} \int_A (z(x, y) - \bar{z})^3 dA, \quad \gamma_1 = \frac{1}{N^2\sigma^3} \sum_{i=1}^N \sum_{j=1}^N (z_{ij} - \bar{z})^3$$

Main characteristics

Integral quantities

- Average of absolute values [l.u.] (profile - R_a , surface - S_a)

$$S_a = \frac{1}{A} \int_A |z(x, y) - \bar{z}| dA, \quad S_a = \frac{1}{N^2} \sum_{i=1}^N \sum_{j=1}^N |z_{ij} - \bar{z}|$$

- Standard deviation of height [l.u.] (σ or R_q for profile, S_q for surface)

$$\sigma = \sqrt{\frac{1}{A} \int_A (z(x, y) - \bar{z})^2 dA}, \quad \sigma = \frac{1}{N} \sqrt{\sum_{i=1}^N \sum_{j=1}^N (z_{ij} - \bar{z})^2}$$

- Maximal valley depth R_v, S_v , maximal peak height R_p, S_p [l.u.]
very sensitive to sample area
- Skewness [adim] (γ_1 or R_{sk}, S_{sk})

$$\gamma_1 = \frac{1}{A\sigma^3} \int_A (z(x, y) - \bar{z})^3 dA, \quad \gamma_1 = \frac{1}{N^2\sigma^3} \sum_{i=1}^N \sum_{j=1}^N (z_{ij} - \bar{z})^3$$

- Kurtosis [adim] (κ or R_{ku}, S_{ku})

$$\kappa = \frac{1}{A\sigma^4} \int_A (z(x, y) - \bar{z})^4 dA, \quad \kappa = \frac{1}{N^2\sigma^4} \sum_{i=1}^N \sum_{j=1}^N (z_{ij} - \bar{z})^4$$

Main characteristics II

Integral quantities II

- Average of absolute value of gradient (slope) [adim] (profile - R_{da} , surface - S_{da})

$$S_{da} = \langle |\nabla z(x, y) - \bar{\nabla}z| \rangle = \frac{1}{A} \int_A |\nabla z(x, y) - \bar{\nabla}z| dA$$
$$S_{da} = \frac{1}{N^2} \sum_{i=1}^N \sum_{j=1}^N \left| \frac{z_{i+1,j} - z_{i,j} - \bar{\Delta z}_x}{\Delta x} \right| + \left| \frac{z_{i,j+1} - z_{i,j} - \bar{\Delta z}_y}{\Delta y} \right|$$

Main characteristics II

Integral quantities II

- Average of absolute value of gradient (slope) [adim] (profile - R_{da} , surface - S_{da})

$$S_{da} = \langle |\nabla z(x, y) - \bar{\nabla} z| \rangle = \frac{1}{A} \int_A |\nabla z(x, y) - \bar{\nabla} z| dA$$
$$S_{da} = \frac{1}{N^2} \sum_{i=1}^N \sum_{j=1}^N \left| \frac{z_{i+1,j} - z_{i,j} - \bar{\Delta z}_x}{\Delta x} \right| + \left| \frac{z_{i,j+1} - z_{i,j} - \bar{\Delta z}_y}{\Delta y} \right|$$

- Standard deviation of gradient (slope) [adim] (profile - R_{dq} , surface - S_{dq})

$$S_{dq} = \sqrt{\langle |\nabla z(x, y) - \bar{\nabla} z|^2 \rangle} = \sqrt{\frac{1}{A} \int_A |\nabla z(x, y) - \bar{\nabla} z|^2 dA}$$
$$S_{dq} = \sqrt{\frac{1}{N^2} \sum_{i=1}^N \sum_{j=1}^N \left| \frac{z_{i+1,j} - z_{i,j} - \bar{\Delta z}_x}{\Delta x} \right|^2 + \left| \frac{z_{i,j+1} - z_{i,j} - \bar{\Delta z}_y}{\Delta y} \right|^2}$$

Main characteristics II

Integral quantities II

- Average of absolute value of gradient (slope) [adim] (profile - R_{da} , surface - S_{da})

$$S_{da} = \langle |\nabla z(x, y) - \bar{\nabla} z| \rangle = \frac{1}{A} \int_A |\nabla z(x, y) - \bar{\nabla} z| dA$$
$$S_{da} = \frac{1}{N^2} \sum_{i=1}^N \sum_{j=1}^N \left| \frac{z_{i+1,j} - z_{i,j} - \bar{\Delta z}_x}{\Delta x} \right| + \left| \frac{z_{i,j+1} - z_{i,j} - \bar{\Delta z}_y}{\Delta y} \right|$$

- Standard deviation of gradient (slope) [adim] (profile - R_{dq} , surface - S_{dq})

$$S_{dq} = \sqrt{\langle |\nabla z(x, y) - \bar{\nabla} z|^2 \rangle} = \sqrt{\frac{1}{A} \int_A |\nabla z(x, y) - \bar{\nabla} z|^2 dA}$$

$$S_{dq} = \sqrt{\frac{1}{N^2} \sum_{i=1}^N \sum_{j=1}^N \left| \frac{z_{i+1,j} - z_{i,j} - \bar{\Delta z}_x}{\Delta x} \right|^2 + \left| \frac{z_{i,j+1} - z_{i,j} - \bar{\Delta z}_y}{\Delta y} \right|^2}$$

- Often in integrated slope measurements a smoothing filter is used, for example, according to ASME B46.1 standard

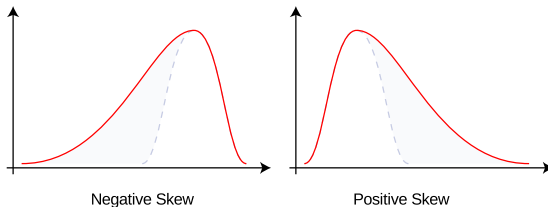
$$\frac{\partial z}{\partial x} \approx \frac{1}{60\Delta x} (z_{i+3,j} - 9z_{i+2,j} + 45z_{i+1,j} - 45z_{i-1,j} + 9z_{i-2,j} - z_{i-3,j})$$

Main characteristics: probability density

- Probability density of heights $P(z)$
- Properties and moments

$$1 = \int_{-\infty}^{\infty} P(z) dz, \quad \bar{z} = \int_{-\infty}^{\infty} zP(z) dz, \quad \sigma = \sqrt{\int_{-\infty}^{\infty} (z - \bar{z})^2 P(z) dz}$$
$$\mu_q = \int_{-\infty}^{\infty} z^q P(z) dz \quad \text{then} \quad \mu_0 = 1, \mu_1 = \bar{z}, \mu_2 = \sigma^2 + \bar{z}^2$$

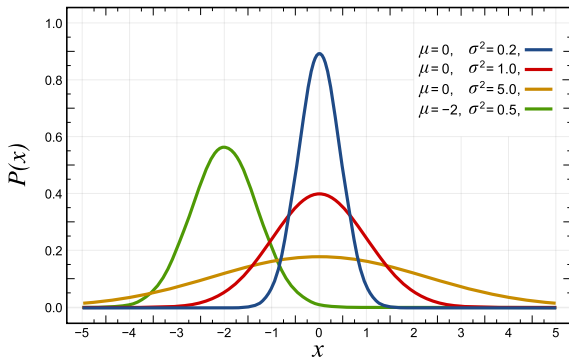
- Link to skewness



Main characteristics: probability density II

Distribution examples

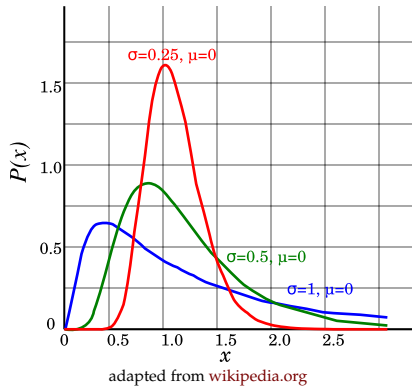
- Normal (Gaussian): $P(x, \mu, \sigma) = \frac{1}{\sigma \sqrt{2\pi}} \exp\left[-\frac{(x - \mu)^2}{2\sigma^2}\right], x \in \mathbb{R}$



Main characteristics: probability density II

Distribution examples

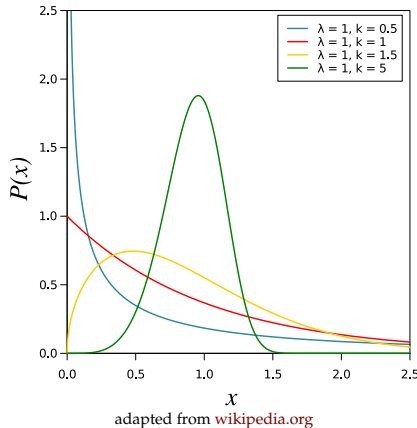
- Lognormal: $P(x, \mu, \sigma) = \frac{1}{x\sigma\sqrt{2\pi}} \exp\left[-\frac{(\log(x) - \mu)^2}{2\sigma^2}\right] x \in \mathbb{R}^+$



Main characteristics: probability density II

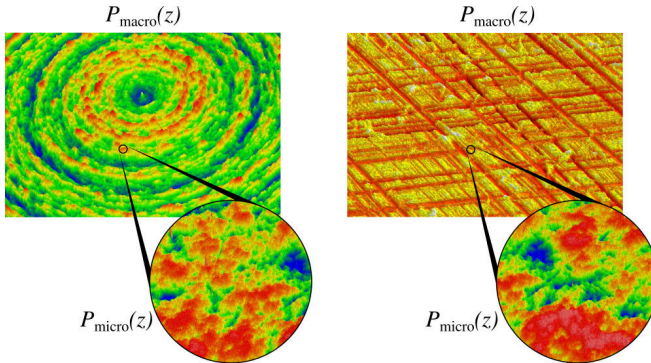
Distribution examples

- Weibull: $P(x, k, \lambda) = \frac{k}{\lambda} \left(\frac{x}{\lambda}\right)^{k-1} \exp^{-(x/\lambda)^k} x \in \mathbb{R}^+$



Real rough surfaces

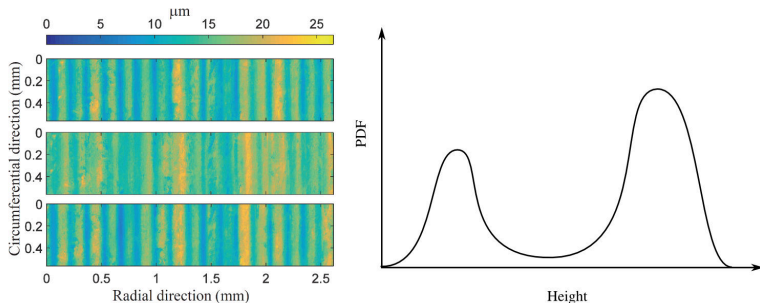
- Turning, scratching, shaping changes macroscopic distribution P_{macro} but might keep microscopic distribution intact P_{micro}
- Wear, polishing, flattening results in removal of the right distribution tail $P(z > z_0) \rightarrow 0$: negative skewness



Macro- and microscopic roughness (left: diamond-turned surface, right: cross-hatched surface)
Images from www.zygo.com used

Real rough surfaces

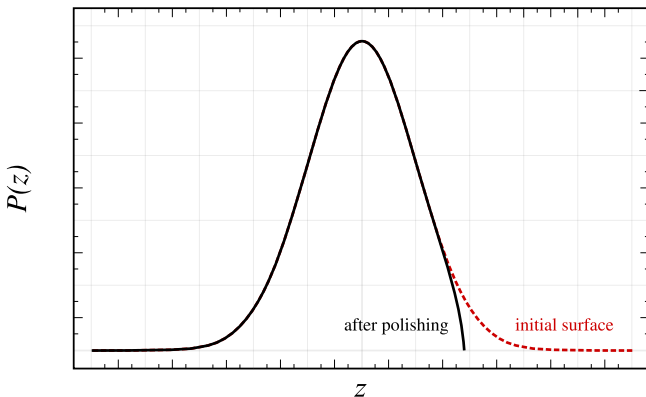
- Turning, scratching, shaping changes macroscopic distribution P_{macro} but might keep microscopic distribution intact P_{micro}
- Wear, polishing, flattening results in removal of the right distribution tail $P(z > z_0) \rightarrow 0$: negative skewness



Turned surface topography and a sketch of height PDF
Pérez-Ràfols, Larsson, Almqvist, Tribol Int 94 (2016)

Real rough surfaces

- Turning, scratching, shaping changes macroscopic distribution P_{macro} but might keep microscopic distribution intact P_{micro}
- Wear, polishing, flattening results in removal of the right distribution tail $P(z > z_0) \rightarrow 0$: negative skewness



Initial surface with Gaussian PDF and surface after polishing

Real rough surfaces

- Turning, scratching, shaping changes macroscopic distribution P_{macro} but might keep microscopic distribution intact P_{micro}
- Wear, polishing, flattening results in removal of the right distribution tail $P(z > z_0) \rightarrow 0$: negative skewness



Very fresh asphalt concrete



Normal asphalt concrete

Real rough surfaces

- Turning, scratching, shaping changes macroscopic distribution P_{macro} but might keep microscopic distribution intact P_{micro}
- Wear, polishing, flattening results in removal of the right distribution tail $P(z > z_0) \rightarrow 0$: negative skewness



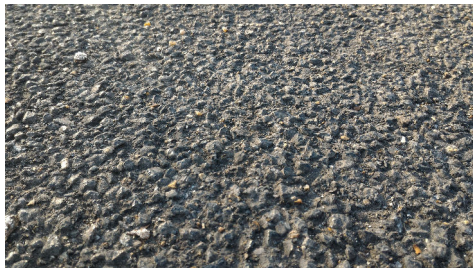
Very fresh asphalt concrete



Normal asphalt concrete . . . with a bolt ☺

Real rough surfaces

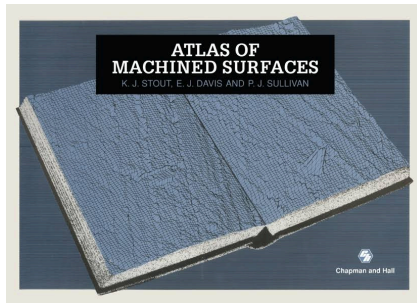
- Turning, scratching, shaping changes macroscopic distribution P_{macro} but might keep microscopic distribution intact P_{micro}
- Wear, polishing, flattening results in removal of the right distribution tail $P(z > z_0) \rightarrow 0$: negative skewness



Old asphalt concrete with worn out bitumen

Real rough surfaces

- Turning, scratching, shaping changes macroscopic distribution P_{macro} but might keep microscopic distribution intact P_{micro}
- Wear, polishing, flattening results in removal of the right distribution tail $P(z > z_0) \rightarrow 0$: negative skewness



Atlas of machined surfaces (with height distributions)

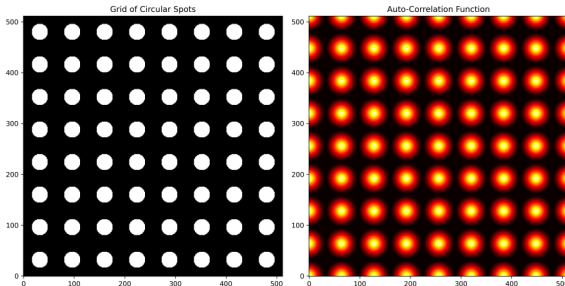
Autocorrelation function

- Continuous autocorrelation function

$$R(\Delta x, \Delta y) = \lim_{L \rightarrow \infty} \frac{1}{L^2} \int_0^L \int_0^L z(x + \Delta x, y + \Delta y) z(x, y) dx dy$$

- Discrete autocorrelation function for a surface $N \times N$

$$R(\Delta x, \Delta y) = \frac{1}{N^2} \sum_{i=0}^{N-1} \sum_{j=0}^{N-1} z(x + \Delta x, y + \Delta y) z(x, y)$$



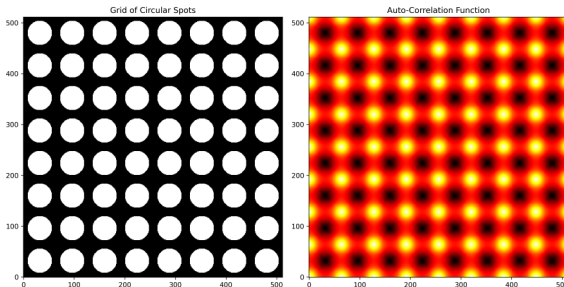
Autocorrelation function

- Continuous autocorrelation function

$$R(\Delta x, \Delta y) = \lim_{L \rightarrow \infty} \frac{1}{L^2} \int_0^L \int_0^L z(x + \Delta x, y + \Delta y) z(x, y) dx dy$$

- Discrete autocorrelation function for a surface $N \times N$

$$R(\Delta x, \Delta y) = \frac{1}{N^2} \sum_{i=0}^{N-1} \sum_{j=0}^{N-1} z(x + \Delta x, y + \Delta y) z(x, y)$$



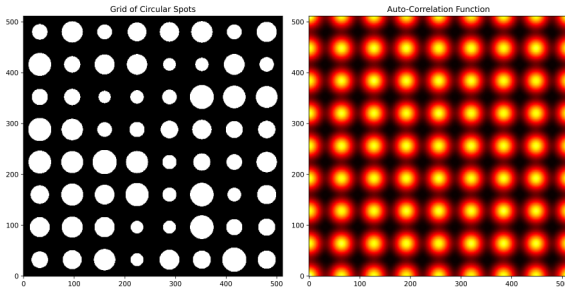
Autocorrelation function

- Continuous autocorrelation function

$$R(\Delta x, \Delta y) = \lim_{L \rightarrow \infty} \frac{1}{L^2} \int_0^L \int_0^L z(x + \Delta x, y + \Delta y) z(x, y) dx dy$$

- Discrete autocorrelation function for a surface $N \times N$

$$R(\Delta x, \Delta y) = \frac{1}{N^2} \sum_{i=0}^{N-1} \sum_{j=0}^{N-1} z(x + \Delta x, y + \Delta y) z(x, y)$$



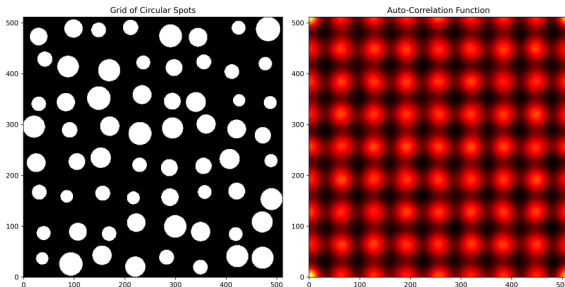
Autocorrelation function

- Continuous autocorrelation function

$$R(\Delta x, \Delta y) = \lim_{L \rightarrow \infty} \frac{1}{L^2} \int_0^L \int_0^L z(x + \Delta x, y + \Delta y) z(x, y) dx dy$$

- Discrete autocorrelation function for a surface $N \times N$

$$R(\Delta x, \Delta y) = \frac{1}{N^2} \sum_{i=0}^{N-1} \sum_{j=0}^{N-1} z(x + \Delta x, y + \Delta y) z(x, y)$$



Power spectral density (PSD)

- Recall: Fourier Transform: $\hat{f}(k) = \frac{1}{2\pi} \int_{-\infty}^{\infty} f(x) \exp(-ikx) dx$
- Recall: Discrete Fourier Transform: $\hat{f}_k = \sum_{n=0}^{N-1} x_n \exp(-ikn/N)$
- where x is the spatial coordinate, $k = 2\pi/\lambda$ is the wavenumber and λ is the wavelength.
- PSD is the Fourier Transform of R
$$\Phi(k_x, k_y) \equiv \hat{R}(k_x, k_y) = \text{FFT} [z(x + \Delta x, y + \Delta y) * z(x, y)]$$
- Using convolution theorem
$$\Phi(k_x, k_y) = \hat{z}(k_x, k_y) \hat{z}^*(k_x, k_y) = \hat{z}^2(k_x, k_y)$$
- Interpretation: energy distribution by frequencies
- Usage: signal analysis, seismology, microstructure characterization, roughness.

Spectral moments

- Spectral moment m_{pq} , $p, q \in \mathbb{N}$:

$$m_{pq} = \iint_{-\infty}^{\infty} k_x^p k_y^q \Phi(k_x, k_y) dk_x dk_y$$

- Generalized spectral moment m_{pq} , $p, q \in \mathbb{R}^+$

- For isotropic surface: $m_2 = m_{20} = m_{02}$, $m_4 = 3m_{22} = m_{40} = m_{04}$

- Averaging:

$$m_2 = \frac{m_{20} + m_{02}}{2}, \quad m_4 = \frac{m_{40} + 3m_{22} + m_{04}}{3}$$

- Physical meaning:

Height variance¹: $m_0 = \langle (z - \langle z \rangle)^2 \rangle$

Gradient variance: $2m_2 = \langle (\nabla z - \langle \nabla z \rangle)^2 \rangle$

Curvature variance: $m_4 = \langle (\nabla \cdot \nabla z - \langle \nabla \cdot \nabla z \rangle)^2 \rangle$

[1] Longuet-Higgins, M. S. (1957). The statistical analysis of a random, moving surface. Phil. Trans. Royal Society of London. Series A 249(966):321-387.

[2] Nayak, P. R. (1971). Random Process Model of Rough Surfaces. Journal of Lubrication Technology, 93(3):398-407

¹Variance is a squared standard deviation

Summary

- Fractal (self-affine) roughness
- Power spectral density (PSD)
 $\Phi(k) \sim k^{-2(H+1)}$

k is a wavenumber,
 H is the Hurst exponent.
- Isotropic/anisotropic surfaces
- Gaussian/non-Gaussian height distribution $P(h)$

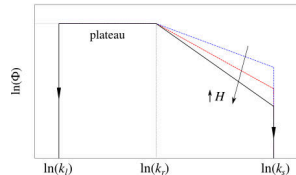
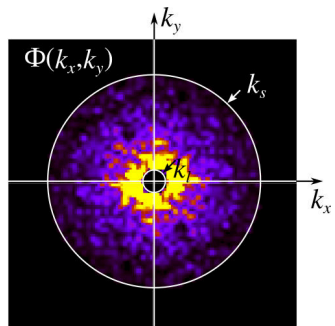


Fig. 3D and radial power spectral densities

Summary

- Fractal (self-affine) roughness
- Power spectral density (PSD)
 $\Phi(k) \sim k^{-2(H+1)}$

k is a wavenumber,
 H is the Hurst exponent.
- Isotropic/anisotropic surfaces
- Gaussian/non-Gaussian height distribution $P(h)$

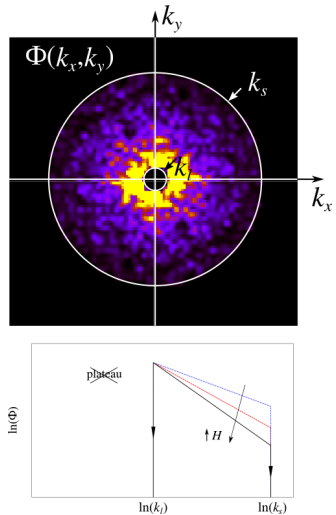


Fig. 3D and radial power spectral densities

Summary

- Fractal (self-affine) roughness
- Power spectral density (PSD)
 $\Phi(k) \sim k^{-2(H+1)}$

k is a wavenumber,

H is the Hurst exponent.

- Isotropic/anisotropic surfaces
- Gaussian/non-Gaussian height distribution $P(h)$

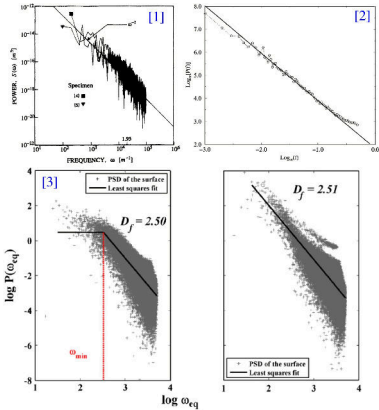


Fig. Power spectral density, measurements

- [1] Majumdar, Tien, Wear 136 (1990)
[2] Schmittbuhl, Jørgen Måløy, Phys. Rev. Lett. 78 (1997)
[3] Vallet, Lasseux, Sainsot, Zahouani, Tribol. Int. 42 (2009)

Summary

- Fractal (self-affine) roughness
- Power spectral density (PSD)
$$\Phi(k) \sim k^{-2(H+1)}$$

k is a wavenumber,
H is the Hurst exponent.
- Isotropic/anisotropic surfaces
- Gaussian/non-Gaussian height distribution $P(h)$

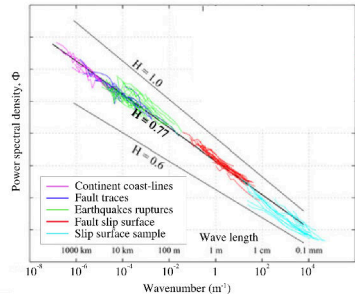


Fig. Power spectral density, geological scales

Adapted from

[4] Renard, Candela, Bouchaud, Geophys. Res. Lett. 40 (2013)

Summary

- Fractal (self-affine) roughness
- Power spectral density (PSD)
 $\Phi(k) \sim k^{-2(H+1)}$

k is a wavenumber,
 H is the Hurst exponent.
- Isotropic/anisotropic surfaces
- Gaussian/non-Gaussian height distribution $P(h)$

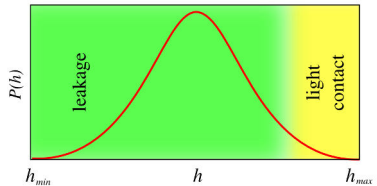


Fig. Height distribution $P(h)$

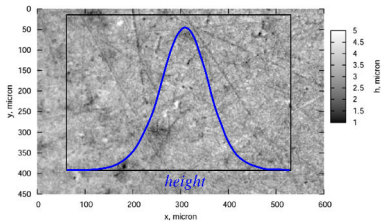


Fig. Height distribution of a polished metal surface

Summary

- Fractal (self-affine) roughness
- Power spectral density (PSD)
 $\Phi(k) \sim k^{-2(H+1)}$

k is a wavenumber,
 H is the Hurst exponent.

- Isotropic/anisotropic surfaces
- Gaussian/non-Gaussian height distribution $P(h)$
- Characteristics:

- $\sqrt{\langle z^2 \rangle}$ - rms heights
- $\sqrt{\langle |\nabla z|^2 \rangle}$ - rms slope (surface gradient)
- $\alpha = m_{00}m_{40}/m_{20}^2$ - breadth of the spectrum (Nayak's parameter^[B]),

$$\text{spectral moments } m_{pq} = \iint_{-\infty}^{\infty} k_x^p k_y^q \Phi(k_x, k_y) dk_x dk_y$$

■ Random process theory

[A] Longuet-Higgins, Philos. Trans. R. Soc. A 250:157 (1957)

[B] Nayak, J. Lub. Tech. (ASME) 93:398 (1973)

[C] Greenwood, Wear 261: 191 (2006)

[D] Borri, Paggi, J. Phys. D Appl Phys 48:045301 (2015)

V.A. Yastrebov

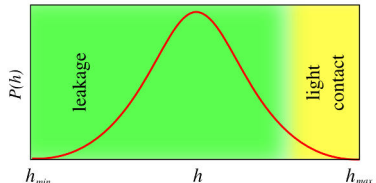


Fig. Height distribution $P(h)$

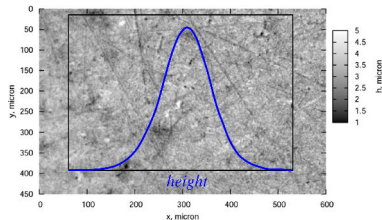


Fig. Height distribution of a polished metal surface

Summary

- Fractal (self-affine) roughness
- Power spectral density (PSD)
$$\Phi(k) \sim k^{-2(H+1)}$$

k is a wavenumber,
 H is the Hurst exponent.

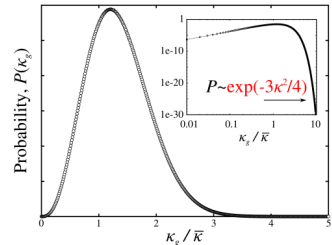
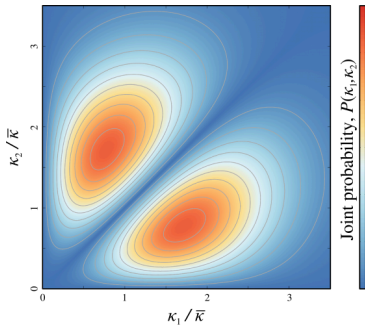
- Isotropic/anisotropic surfaces
- Gaussian/non-Gaussian height distribution $P(h)$
- Characteristics:

- $\sqrt{\langle z^2 \rangle}$ - rms heights
- $\sqrt{\langle |\nabla z|^2 \rangle}$ - rms slope (surface gradient)
- $\alpha = m_{00}m_{40}/m_{20}^2$ - breadth of the spectrum (Nayak's parameter^[B]),

$$\text{spectral moments } m_{pq} = \iint_{-\infty}^{\infty} k_x^p k_y^q \Phi(k_x, k_y) dk_x dk_y$$

■ Random process theory

- [A] Longuet-Higgins, Philos. Trans. R. Soc. A 250:157 (1957)
[B] Nayak, J. Lub. Tech. (ASME) 93:398 (1973)
[C] Greenwood, Wear 261: 191 (2006)
[D] Borri, Paggi, J. Phys. D Appl Phys 48:045301 (2015)
V.A. Yastrebov



$$P \sim \kappa^2 \exp(-3\kappa^2/4) \operatorname{erf}(3\kappa/2)$$

Distribution of asperity curvatures

Summary

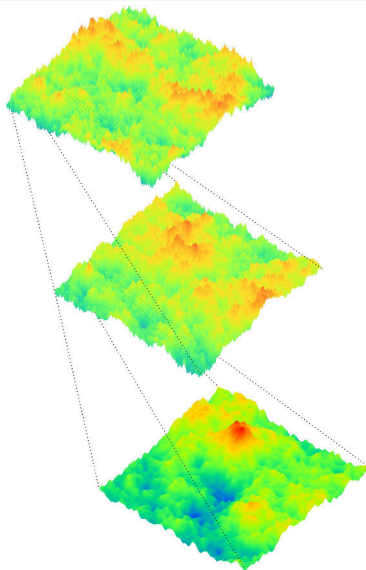


Fig. Example of a rough surface for $H = 0.3$

Recall: the Hurst exponent H and the fractal dimension D in 2D space are interconnected via $D = 3 - H$

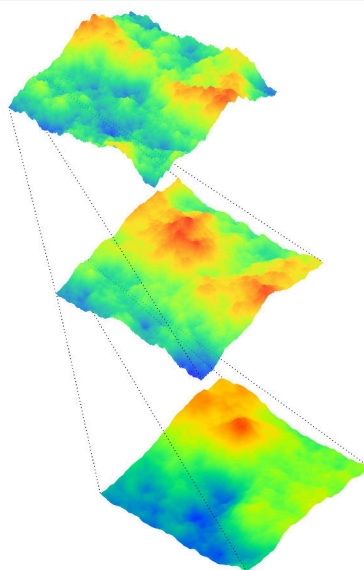
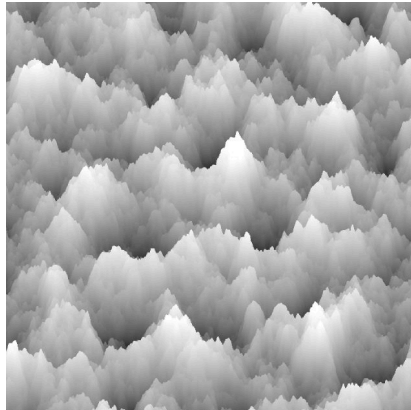


Fig. Example of a rough surface for $H = 0.8$



Flight over a rough surface

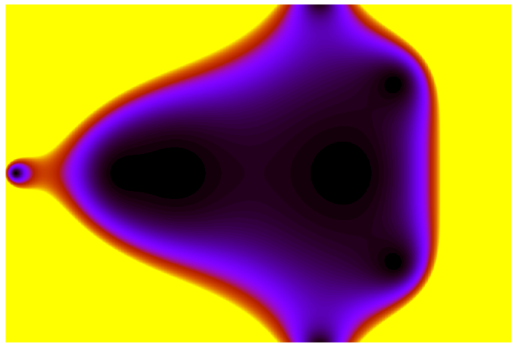


Romanesco broccoli

Fractals

- Mandelbrot set (not a fractal)
- Recursive function

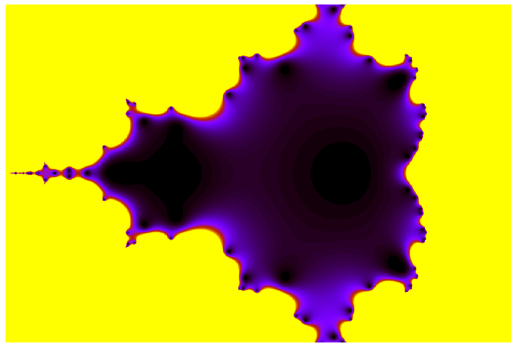
$$z_{i+1} = z_i^2 + z, \quad z \in \mathbb{C}$$



Fractals

- Mandelbrot set (not a fractal)
- Recursive function

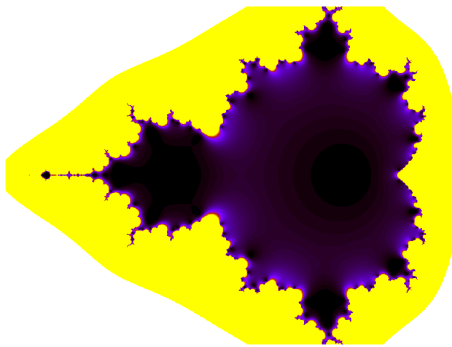
$$z_{i+1} = z_i^2 + z, \quad z \in \mathbb{C}$$



Fractals

- Mandelbrot set (not a fractal)
- Recursive function

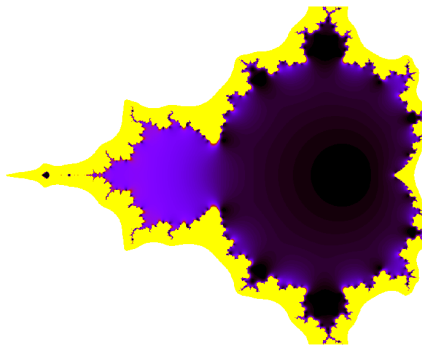
$$z_{i+1} = z_i^2 + z, \quad z \in \mathbb{C}$$



Fractals

- Mandelbrot set (not a fractal)
- Recursive function

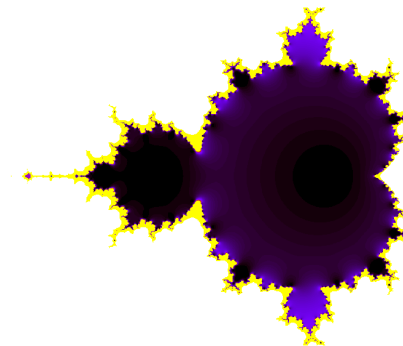
$$z_{i+1} = z_i^2 + z, \quad z \in \mathbb{C}$$



Fractals

- Mandelbrot set (not a fractal)
- Recursive function

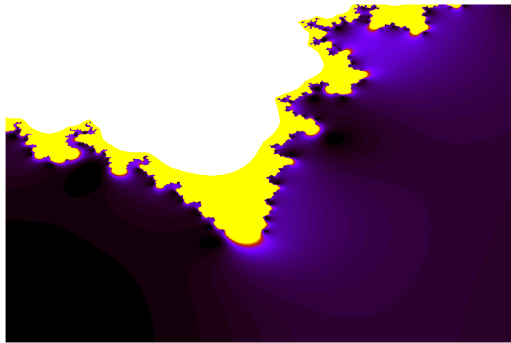
$$z_{i+1} = z_i^2 + z, \quad z \in \mathbb{C}$$



Fractals

- Mandelbrot set (not a fractal)
- Recursive function

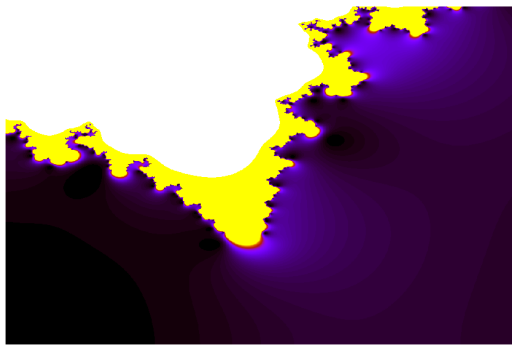
$$z_{i+1} = z_i^2 + z, \quad z \in \mathbb{C}$$



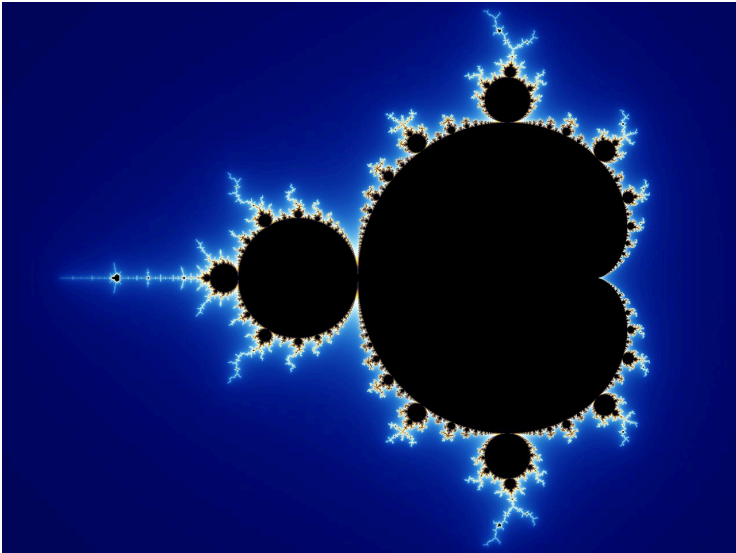
Fractals

- Mandelbrot set (not a fractal)
- Recursive function

$$z_{i+1} = z_i^2 + z, \quad z \in \mathbb{C}$$

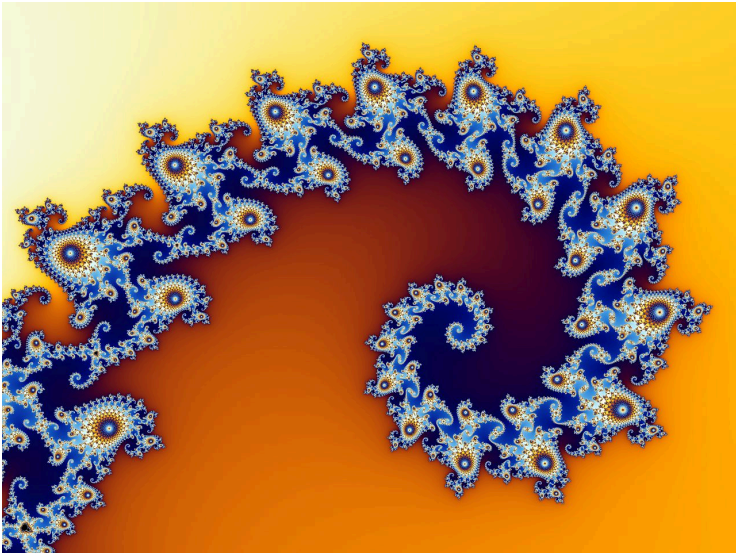


Fractals



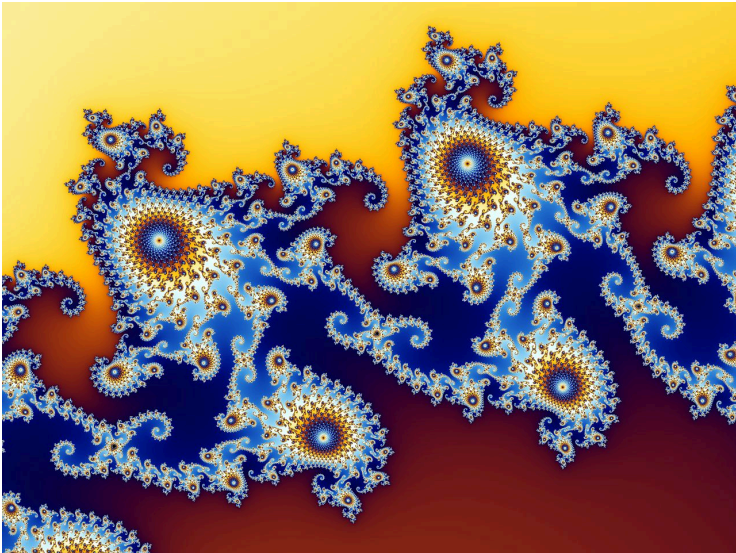
Mandelbrot set ([Wikipedia](#))

Fractals



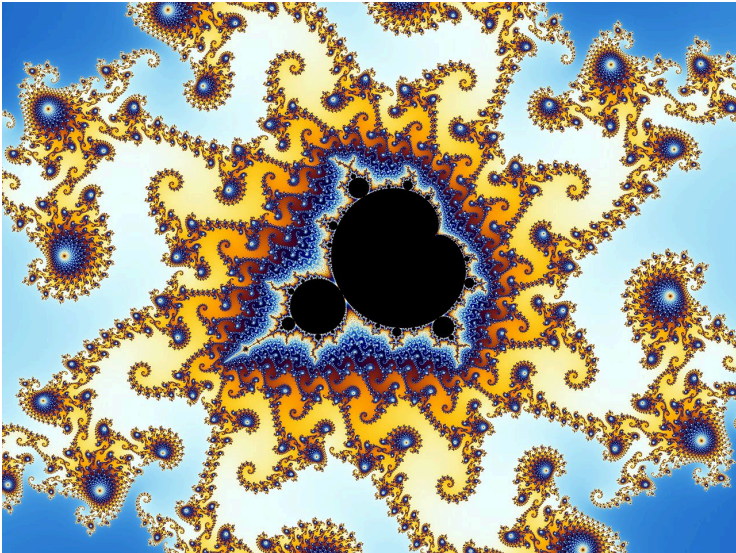
Element of Mandelbrot set ([Wikipedia](#))

Fractals



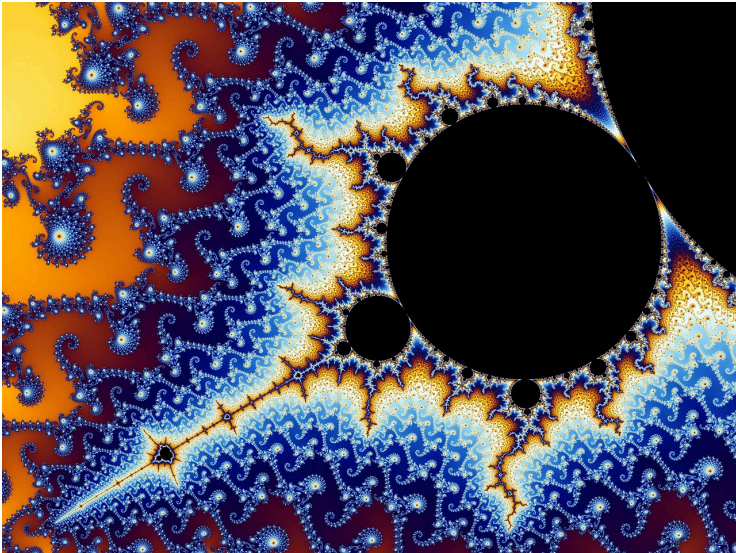
Element of Mandelbrot set ([Wikipedia](#))

Fractals



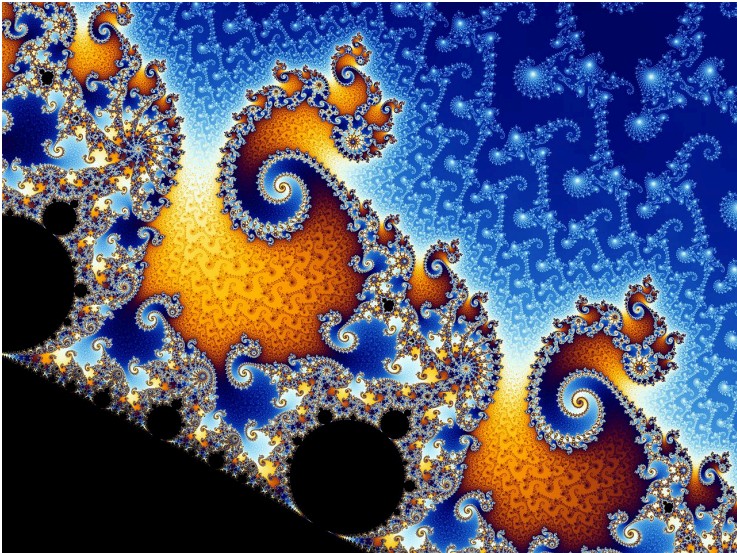
Element of Mandelbrot set ([Wikipedia](#))

Fractals



Element of Mandelbrot set ([Wikipedia](#))

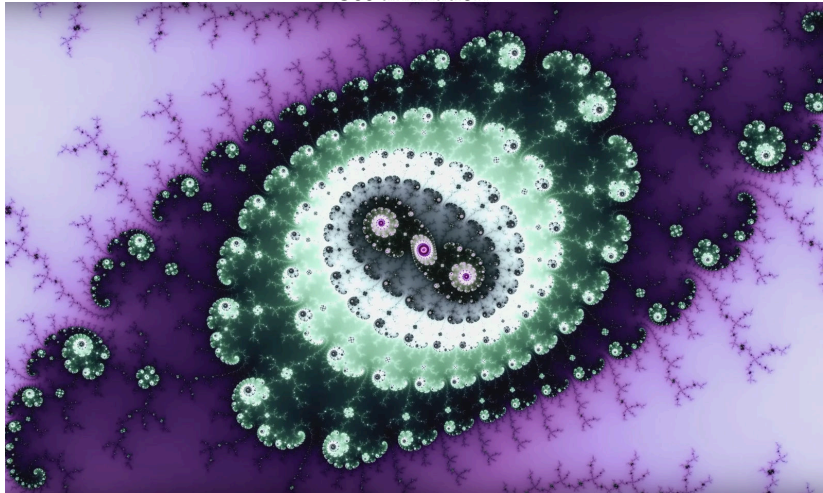
Fractals



Element of Mandelbrot set ([Wikipedia](#))

Fractals

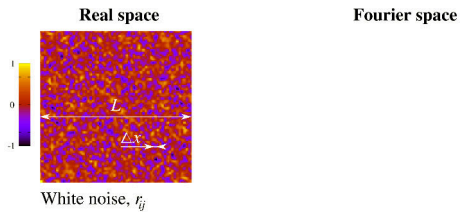
See animation



<https://youtu.be/pCpLWbHVNhk>

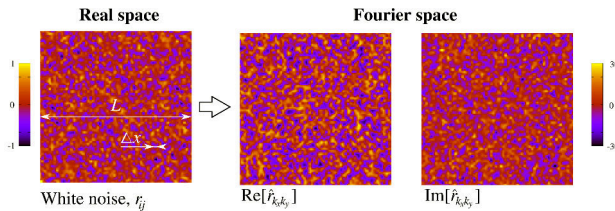
70 minutes of 4K "Eye of the Universe - Mandelbrot Fractal Zoom" e^{1091}

Synthesized rough surfaces: in pictures



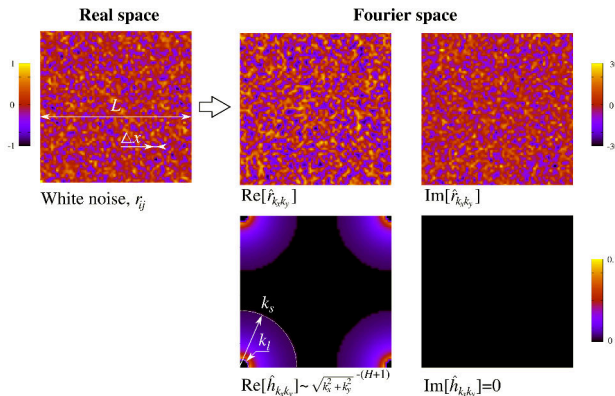
[1] Y. Z. Hu and K. Tonder, Int. J. Machine Tools Manuf. 32, 83 (1992)

Synthesized rough surfaces: in pictures



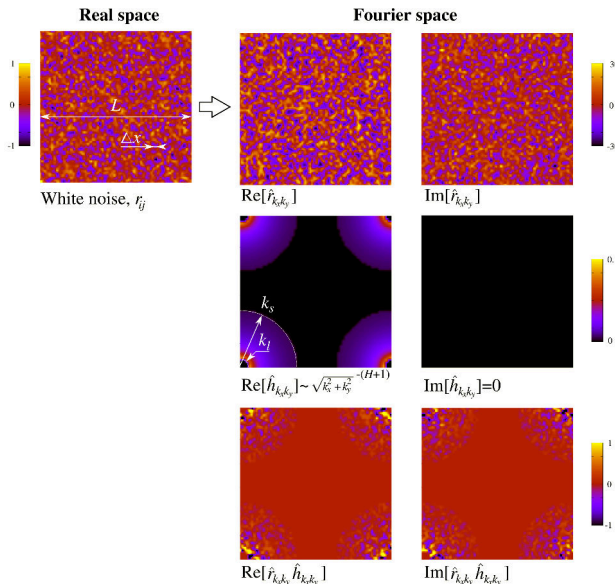
[1] Y. Z. Hu and K. Tonder, Int. J. Machine Tools Manuf. 32, 83 (1992)

Synthesized rough surfaces: in pictures



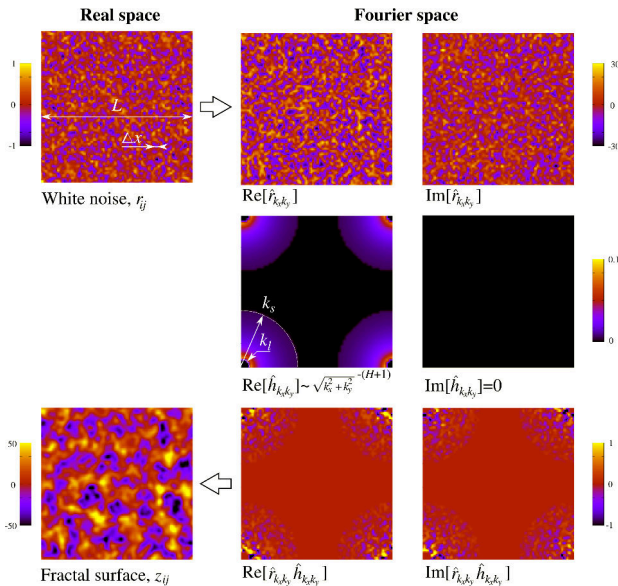
[1] Y. Z. Hu and K. Tonder, Int. J. Machine Tools Manuf. 32, 83 (1992)

Synthesized rough surfaces: in pictures



[1] Y. Z. Hu and K. Tonder, Int. J. Machine Tools Manuf. 32, 83 (1992)

Synthesized rough surfaces: in pictures



[1] Y. Z. Hu and K. Tonder, Int. J. Machine Tools Manuf. 32, 83 (1992)

Synthesized rough surfaces: in equations

- White noise:

$$w(x_i, y_j), \quad \langle w \rangle = 0, \quad \langle w^2 \rangle = \Phi_0$$

- Transform in Fourier space:

$$\hat{w}_{ij} = \hat{w}(k_x, k_y) = \sum_{i=0}^{N-1} \sum_{j=0}^{N-1} w(x_i, y_j) \exp[-i(k_x x_i + k_y y_j)], \quad \langle \hat{w} \hat{w}^* \rangle = \langle w^2 \rangle = \Phi_0$$

- Create a filter

$$\hat{f}_{ij} = \hat{f}(k_x, k_y) = \begin{cases} \left[\frac{K_x^2 + K_y^2}{k_l^2} \right]^{-(1+H)/2}, & \text{for } 1 \leq \frac{\sqrt{K_x^2 + K_y^2}}{k_l} \leq \zeta \\ 0, & \text{elsewhere,} \end{cases},$$

where $K_x = (s+1)\pi/L - sk_x$, $K_y = (t+1)\pi/L - tk_y$ for $s, t \in \{-1, 1\}$, $\zeta = k_s/k_l$

- Filter white noise:

$$\hat{z}_{ij} = \hat{z}(k_x, k_y) = \Re(\hat{f}_{ij}) [\Re(\hat{w}_{ij}) + i \Im(\hat{w}_{ij})]$$

- Back to real space:

$$z(x_i, y_j) = \sum_{l=0}^{N-1} \sum_{m=0}^{N-1} \hat{z}_{lm} \exp[i2\pi(lx_i + my_j)/L]$$

Synthesized rough surfaces: in equations II

- Power spectral density:

$$\Phi(k_x, k_y) = \hat{z}(k_x, k_y)\hat{z}^*(k_x, k_y) = \hat{f}^2(k_x, k_y)\hat{w}^2(k_x, k_y)$$

- Averaging over multiple samples:

$$\langle \Phi(k_x, k_y) \rangle = \langle \hat{w}^2(k_x, k_y) \rangle \hat{f}^2(k_x, k_y) = \begin{cases} \Phi_0 \left[\frac{\sqrt{k_x^2 + k_y^2}}{k_l} \right]^{-2(1+H)}, & \text{for } 1 \leq \frac{\sqrt{k_x^2 + k_y^2}}{k_l} \leq \zeta \\ 0, & \text{elsewhere,} \end{cases}$$

- For isotropic surface:

$$\langle \Phi(K) \rangle = \begin{cases} \Phi_0 (K/k_l)^{-2(1+H)}, & \text{if } 1 \leq K/k_l \leq \zeta \\ 0, & \text{otherwise.} \end{cases}$$

Effect of parameters: illustration

- Effect of the high frequency cutoff k_s

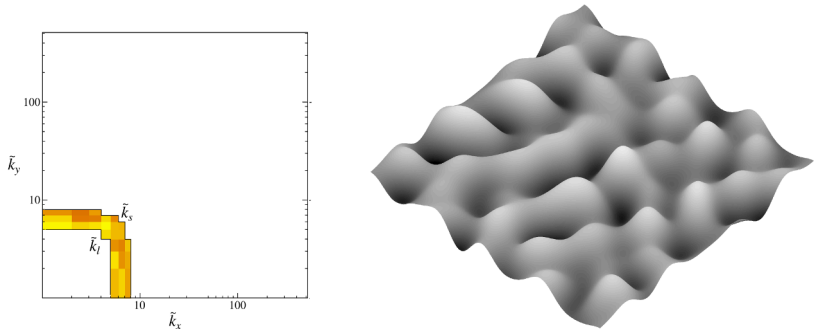


Fig. Power spectral density (Fourier space)
and corresponding rough surface (real space) for
 $k_l = 4, k_s = 8$

Effect of parameters: illustration

- Effect of the high frequency cutoff k_s

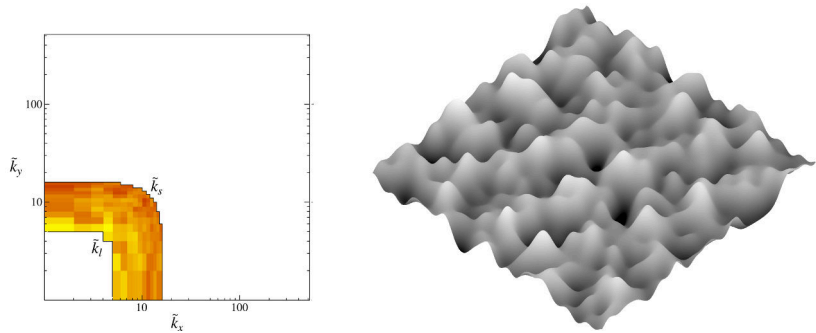


Fig. Power spectral density (Fourier space)
and corresponding rough surface (real space) for
 $k_l = 4, \quad k_s = 16$

Effect of parameters: illustration

- Effect of the high frequency cutoff k_s

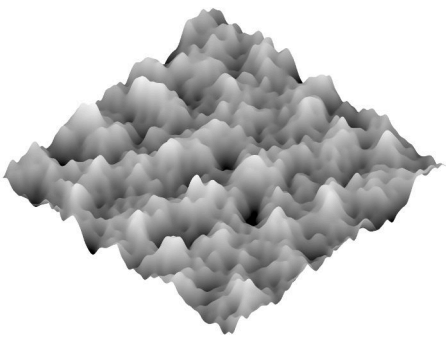
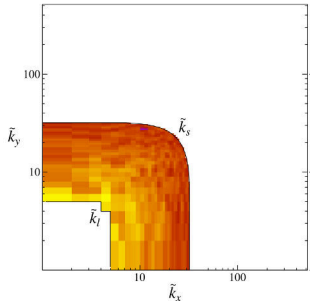


Fig. Power spectral density (Fourier space)
and corresponding rough surface (real space) for
 $k_l = 4, k_s = 32$

Effect of parameters: illustration

- Effect of the high frequency cutoff k_s

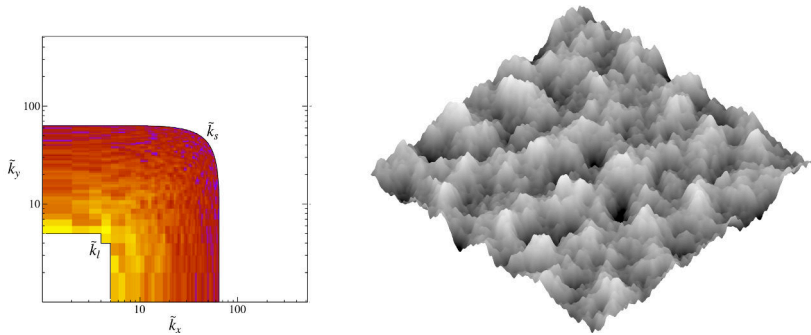


Fig. Power spectral density (Fourier space)
and corresponding rough surface (real space) for
 $k_l = 4, k_s = 64$

Effect of parameters: illustration

- Effect of the high frequency cutoff k_s

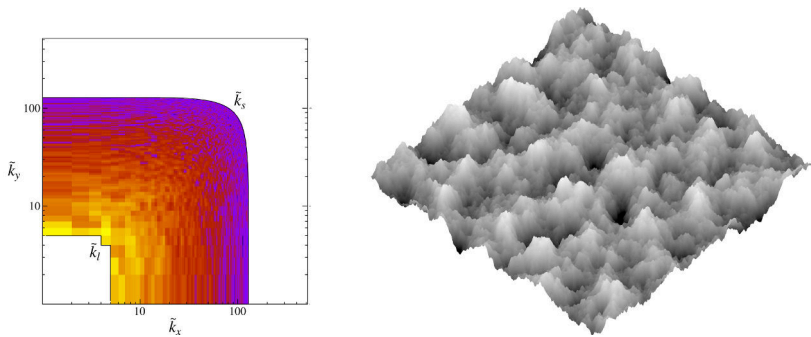


Fig. Power spectral density (Fourier space)
and corresponding rough surface (real space) for
 $k_l = 4, k_s = 128$

Effect of parameters: illustration

- Effect of the lower frequency cutoff k_l for $k_s/k_l = \text{const}$

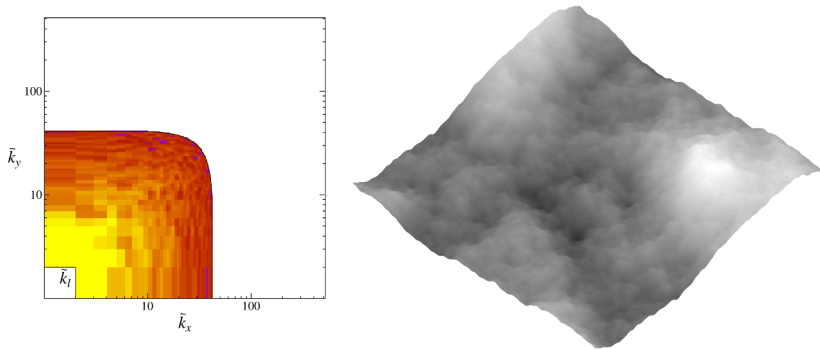


Fig. Power spectral density (Fourier space)
and corresponding rough surface (real space) for
 $k_l = 1, k_s = 43$

Effect of parameters: illustration

- Effect of the lower frequency cutoff k_l for $k_s/k_l = \text{const}$

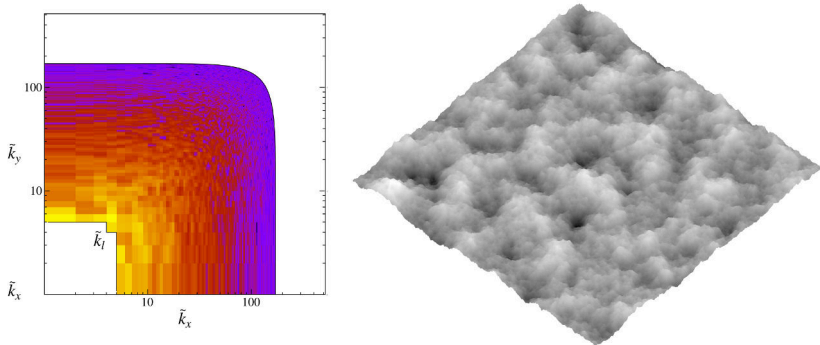


Fig. Power spectral density (Fourier space)
and corresponding rough surface (real space) for
 $k_l = 4, k_s = 171$

Effect of parameters: illustration

- Effect of the lower frequency cutoff k_l for $k_s/k_l = \text{const}$

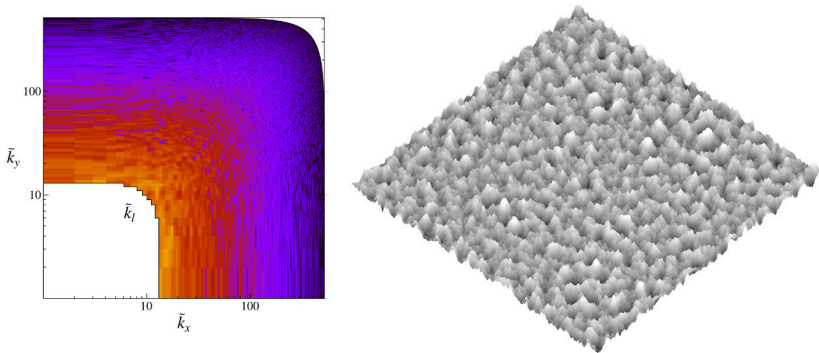


Fig. Power spectral density (Fourier space)
and corresponding rough surface (real space) for
 $k_l = 12, k_s = 512$

Effect of parameters: illustration

- Effect of the ratio of the higher cutoff to the discretization k_s/N

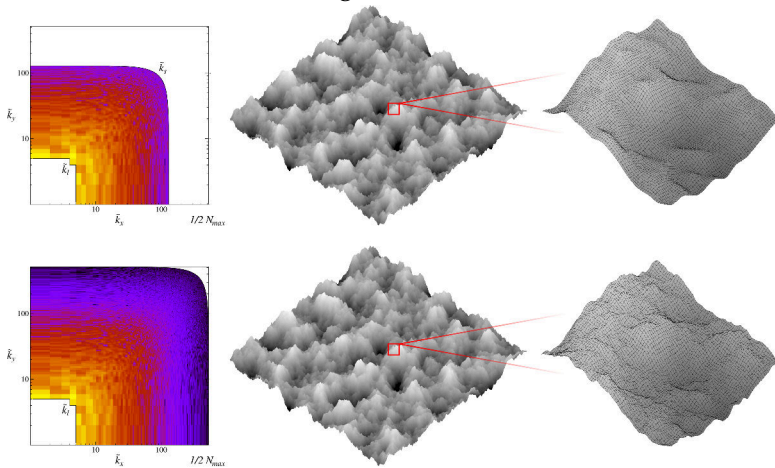


Fig. Power spectral densities (Fourier space)
and corresponding rough surfaces (real space) for
 $k_l = 12, k_s/N = 1/8$ **VS** $k_l = 12, k_s/N = 1/2$

Effect of parameters: illustration

- Effect of the ratio of the higher cutoff to the discretization k_s/N

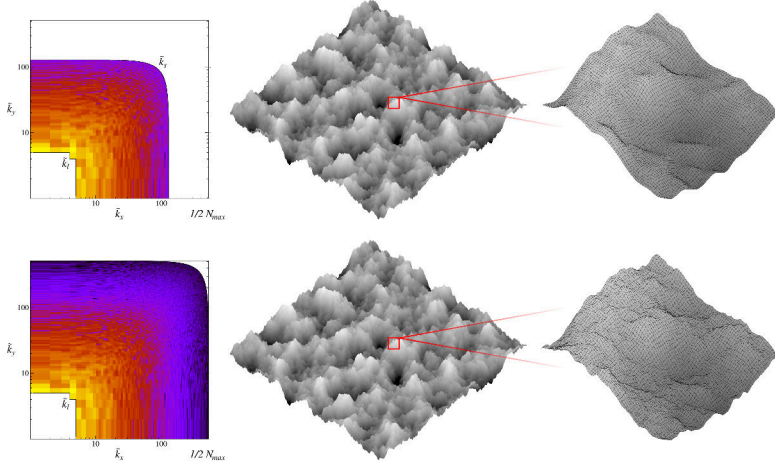


Fig. Power spectral densities (Fourier space) and corresponding rough surfaces (real space) for
 $k_l = 12, k_s/N = 1/8$ (fine) VS $k_l = 12, k_s/N = 1/2$ (too coarse)
for mechanical simulations

Effect of parameters: illustration

- Effect of the discretisation (single asperity)

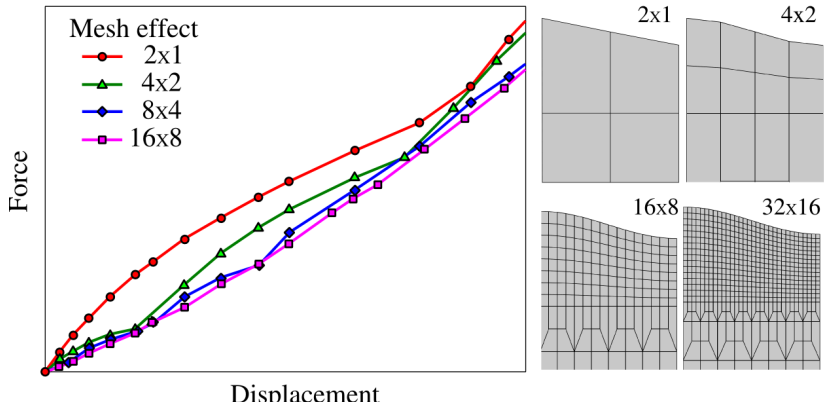
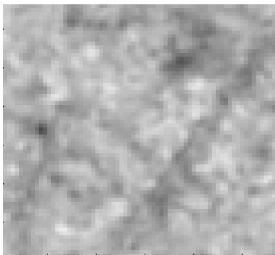


Fig. Effect of the mesh on mechanical response

Effect of parameters: illustration

- Data interpolation (Shanon, bi-cubic Bézier surfaces)

Experimental



Smoothed (enriched)

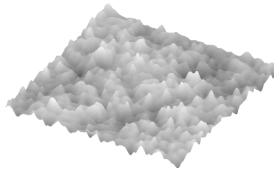
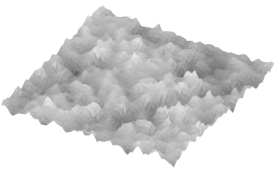
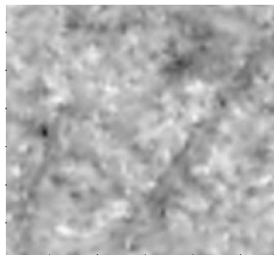


Fig. Bi-cubic Bézier interpolation of an experimental rough surface

[1] Hyun, Robbins, Tribol. Int. (2007)

[2] Yastrebov, Durand, Proudhon, Cailletaud, C.R. Mécan. (2011)

Effect of parameters

Effect of parameters:

- k_l low frequency cutoff
 - *representativity/normality*^[1,2,3]
- k_s high frequency cutoff
 - *smoothness and density of asperities*
- $\zeta = k_s/k_l$ ratio^[3]
 - *breadth of the spectrum*

$$\alpha \sim \zeta^{2H}$$

Nayak's parameter α is the central characteristic of roughness in asperity based mechanical models.

- [1] Vallet, Lasseux, Sainsot, Zahouani, Tribol. Int. (2009)
- [2] Yastrebov, Durand, Proudhon, Cailletaud, C.R. Mécan. (2011)
- [3] Yastrebov, Anciaux, Molinari, Phys. Rev. E (2012)
- [4] Yastrebov, Anciaux, Molinari, Int. J. Solids Struct. (2015)

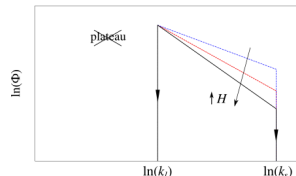
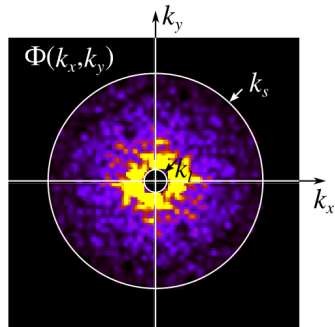


Fig. 3D and radial power spectral densities

Effect of parameters

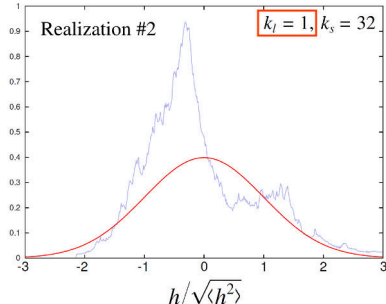
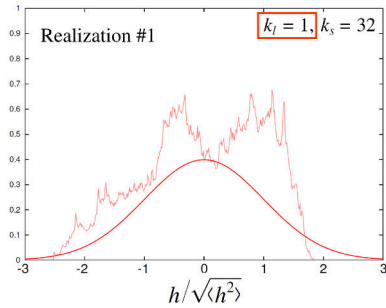
Effect of parameters:

- k_l low frequency cutoff
 - *representativity/normality*^[1,2,3]
- k_s high frequency cutoff
 - *smoothness and density of asperities*
- $\zeta = k_s/k_l$ ratio^[3]
 - *breadth of the spectrum*

$$\alpha \sim \zeta^{2H}$$

Nayak's parameter α is the central characteristic of roughness in asperity based mechanical models.

- [1] Vallet, Lasseux, Sainsot, Zahouani, Tribol. Int. (2009)
- [2] Yastrebov, Durand, Proudhon, Cailletaud, C.R. Mécan. (2011)
- [3] Yastrebov, Anciaux, Molinari, Phys. Rev. E (2012)
- [4] Yastrebov, Anciaux, Molinari, Int. J. Solids Struct. (2015)



Effect of parameters

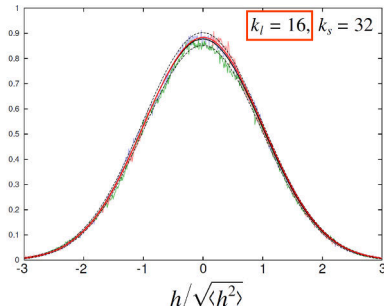
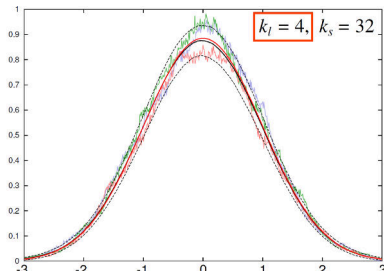
Effect of parameters:

- k_l low frequency cutoff
 - *representativity/normality*^[1,2,3]
- k_s high frequency cutoff
 - *smoothness and density of asperities*
- $\zeta = k_s/k_l$ ratio^[3]
 - *breadth of the spectrum*

$$\alpha \sim \zeta^{2H}$$

Nayak's parameter α is the central characteristic of roughness in asperity based mechanical models.

- [1] Vallet, Lasseux, Sainsot, Zahouani, Tribol. Int. (2009)
- [2] Yastrebov, Durand, Proudhon, Cailletaud, C.R. Mécan. (2011)
- [3] Yastrebov, Anciaux, Molinari, Phys. Rev. E (2012)
- [4] Yastrebov, Anciaux, Molinari, Int. J. Solids Struct. (2015)



Interconnection of parameters

- Spectral moment and k_l, k_s, H :

$$m_{0p} \approx m_{p0} \approx \Phi_0 \int_{k_l}^{k_s} \int_0^{2\pi} [k \cos(\varphi)]^p (k/k_l)^{-2(1+H)} k dk d\varphi = \Phi_0 k_l^{p+2} \frac{\zeta^{p-2H} - 1}{p - 2H} T(p)$$

$$\text{with } T(p) = \int_0^{2\pi} \cos^p(\varphi) d\varphi = \begin{cases} 2\pi, & \text{if } p = 0; \\ \pi, & \text{if } p = 2; \\ 3\pi/4, & \text{if } p = 4. \end{cases}$$

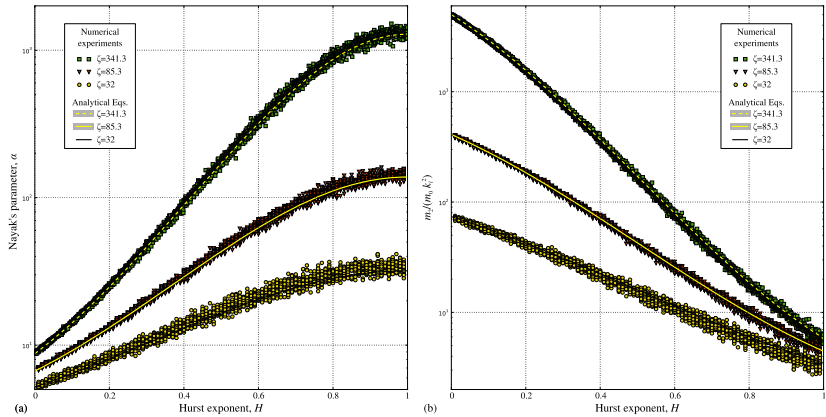
- Nayak's parameter

$$\alpha(H, \zeta) = \frac{3}{2} \frac{(1-H)^2}{H(H-2)} \frac{(\zeta^{-2H} - 1)(\zeta^{4-2H} - 1)}{(\zeta^{2-2H} - 1)^2}$$

- Asperity density

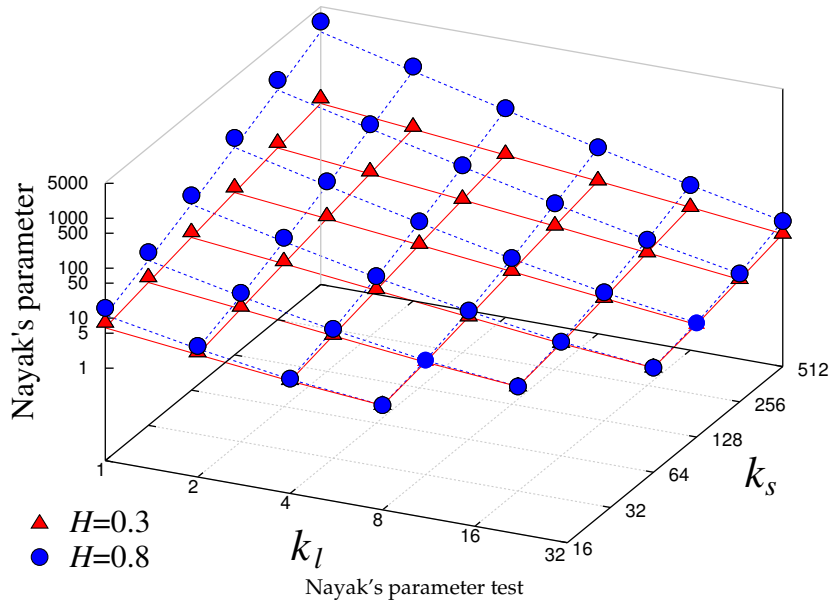
$$D = \frac{\sqrt{3}}{18\pi} \frac{m_4}{m_2} = \frac{\sqrt{3}}{24\pi} \frac{1-H}{2-H} \frac{\zeta^{4-2H} - 1}{\zeta^{2-2H} - 1} k_l^2$$

Interconnection of parameters

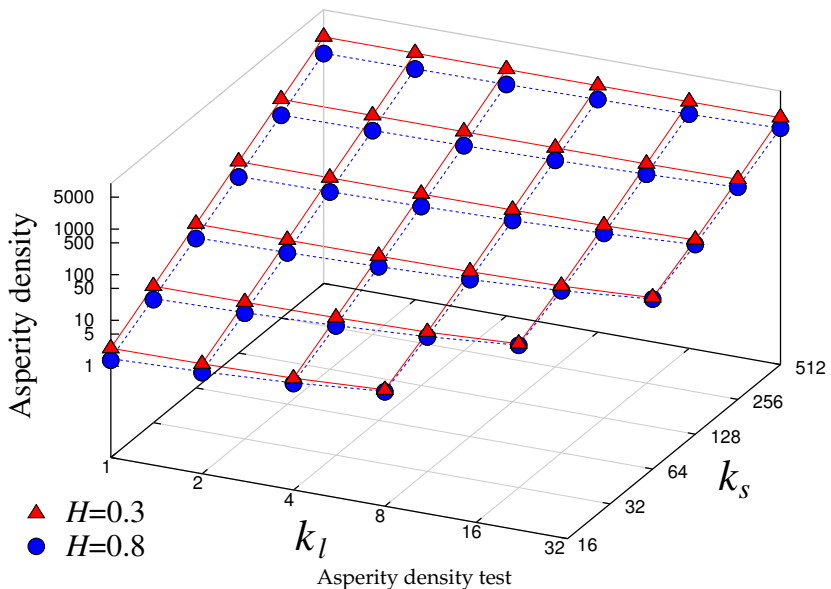


Numerical verification on 100 000 generated rough surfaces with 2048×2048 points

Interconnection of parameters



Interconnection of parameters



Asperity analysis

- Detect summits (z_{ij} higher than neighbouring points) and evaluate second derivatives

$$\frac{\partial^2 z}{\partial x^2} = \frac{z_{i+1j} + z_{i-1j} - 2z_{ij}}{2\Delta x^2}; \quad \frac{\partial^2 z}{\partial y^2} = \frac{z_{i+1j} + z_{i-1j} - 2z_{ij}}{2\Delta x^2}$$
$$\frac{\partial^2 z}{\partial x \partial y} = \frac{z_{i+1j+1} + z_{i+1j-1} - z_{i-1j-1} - z_{i-1j+1}}{4\Delta x^2}$$

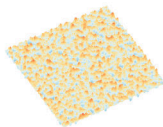
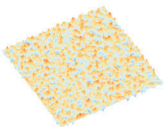
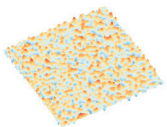
- Principal curvatures $\kappa_{1,2}$:

$$\kappa_{1,2} = \frac{1}{2} \left(\frac{\partial^2 z}{\partial x^2} + \frac{\partial^2 z}{\partial y^2} \right) \pm \sqrt{\left(\frac{\partial^2 z}{\partial x \partial y} \right)^2 + \frac{1}{4} \left(\frac{\partial^2 z}{\partial x^2} - \frac{\partial^2 z}{\partial y^2} \right)^2}$$

- Saddle point $\kappa_1 \kappa_2 < 0$, extrema $\kappa_1 \kappa_2 > 0$

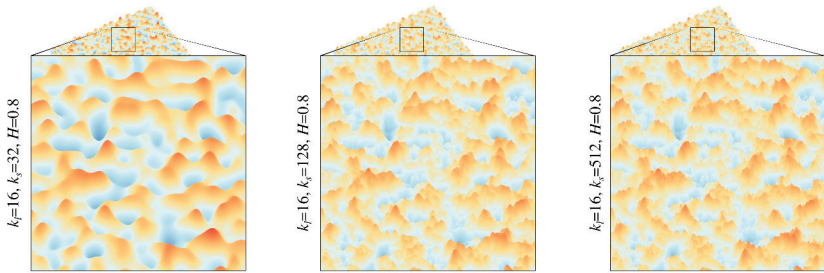
- Mean curvature which can be safely used in Hertz theory: $\bar{\kappa} = \sqrt{\kappa_1 \kappa_2}$

Asperity analysis



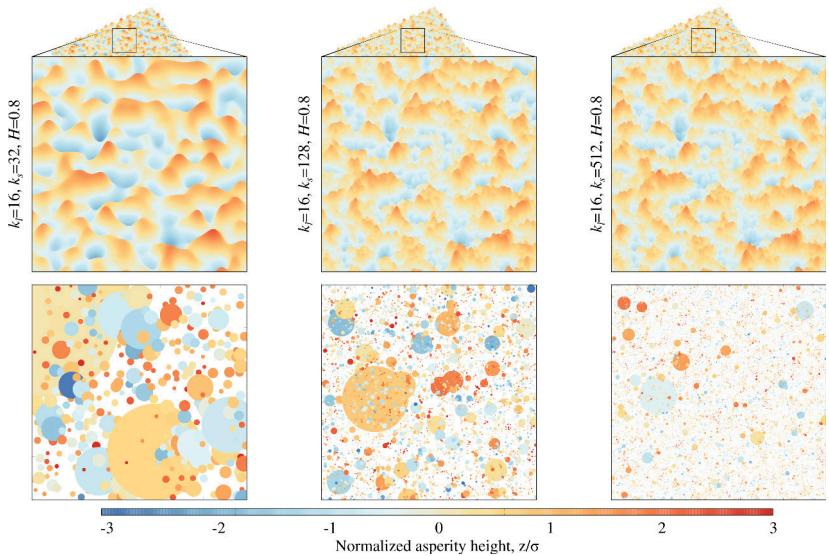
Rough surfaces and associated asperities

Asperity analysis



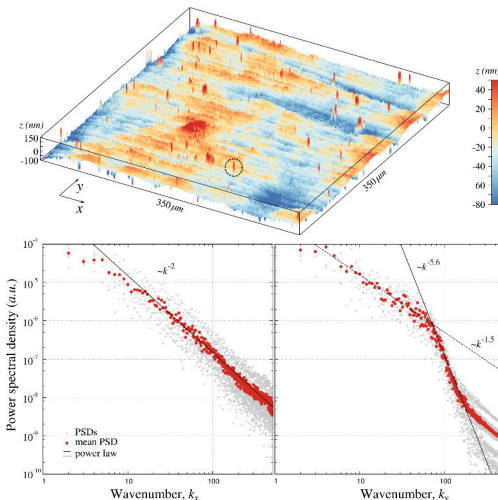
Rough surfaces and associated asperities

Asperity analysis



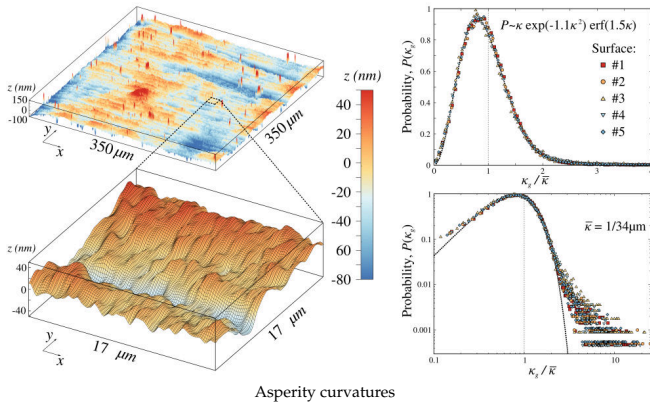
Rough surfaces and associated asperities

Examples

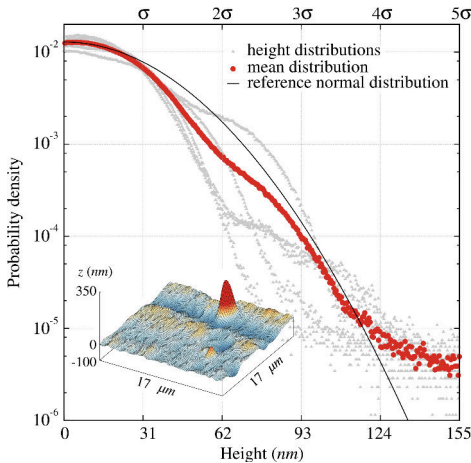


[1] Yastrebov et al, Three-level multi-scale modeling of electrical contacts sensitivity study and experimental validation, Proceedings of Holm Conference, 2015.

Examples



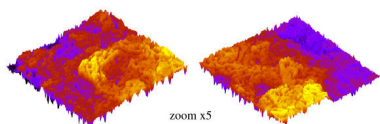
Examples



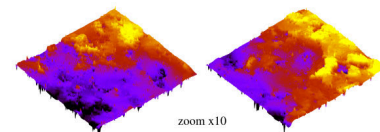
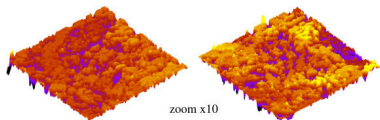
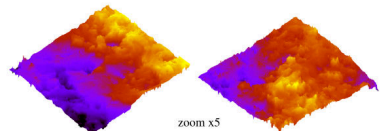
[1] Yastrebov et al, Three-level multi-scale modeling of electrical contacts sensitivity study and experimental validation, Proceedings of Holm Conference, 2015.

Examples

Bright fracture surface

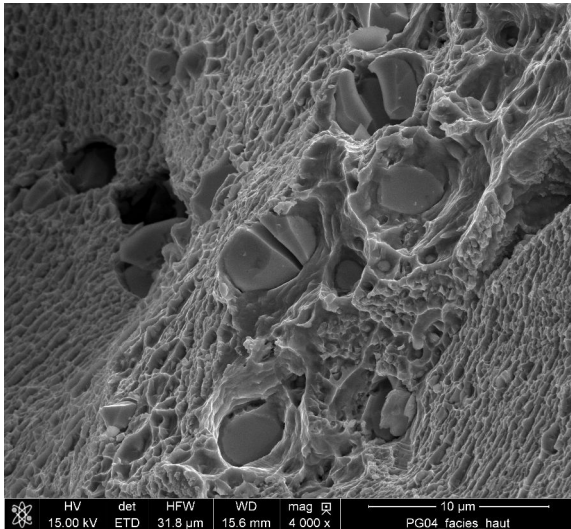


Dark fracture surface



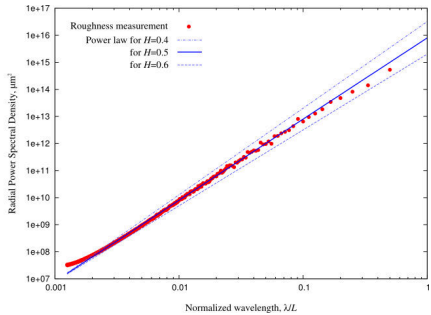
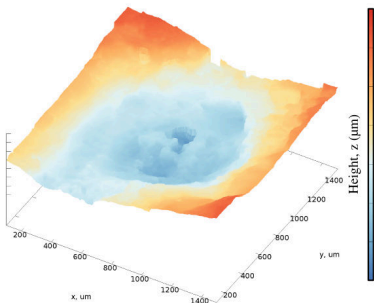
Fatigue & creep fracture surfaces (Ti-alloy)
in collaboration with A. Marchenko

Examples



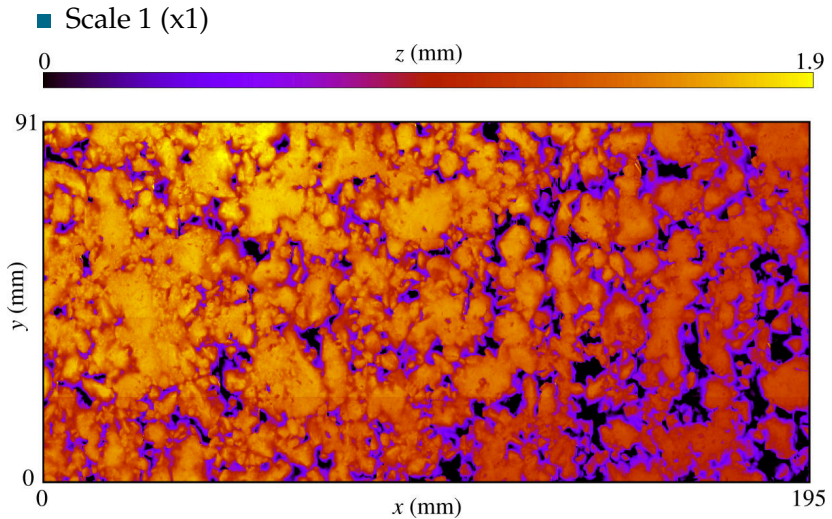
Fatigue fracture surface (Co-alloy), particles WC
Courtesy of V. Esin

Examples



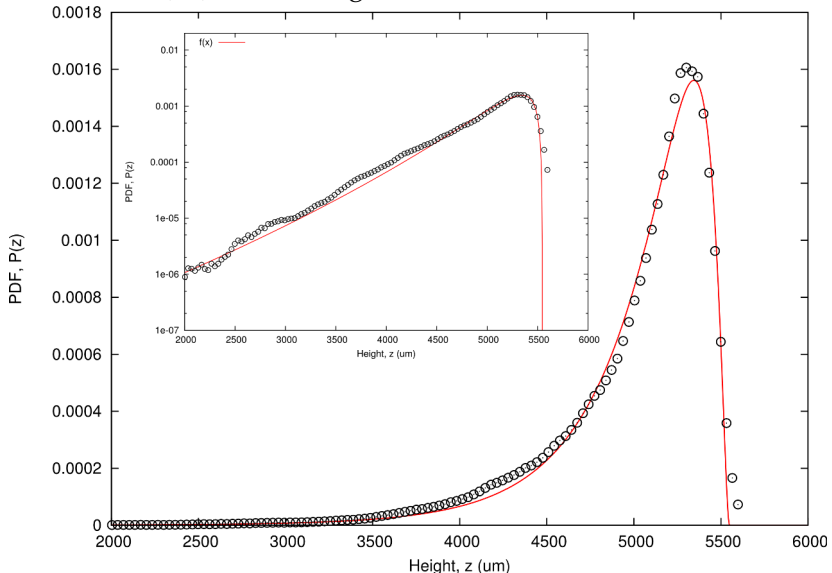
Crater topography and PSD
In collaboration with D. Tkalich (NTNU, Sintef)

Multiscale road roughness

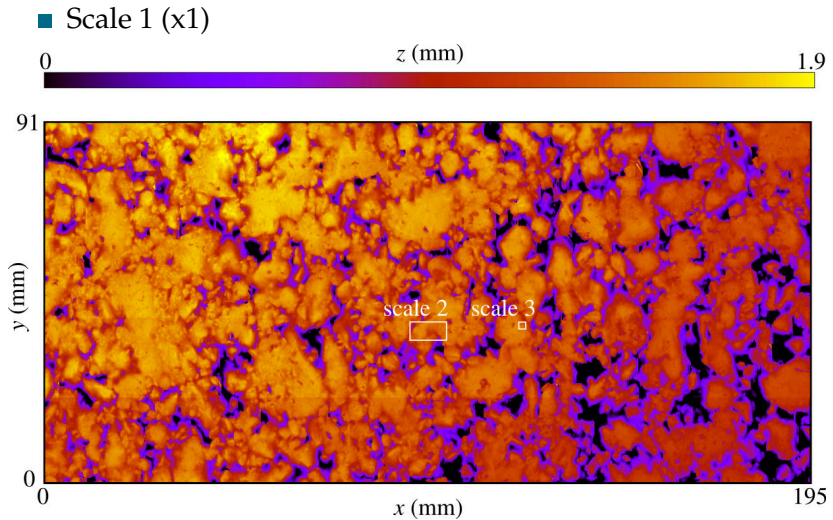


Multiscale road roughness

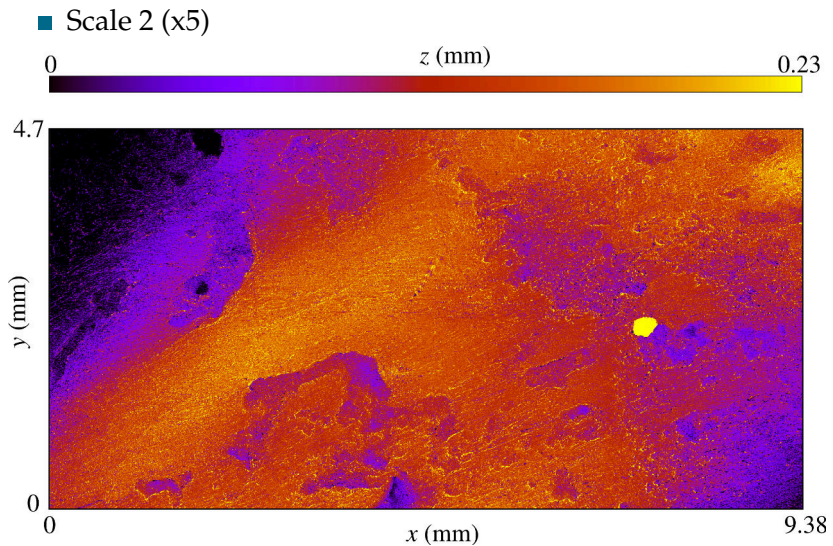
■ Scale 1 (x1): PDF and generalized Weibull fit



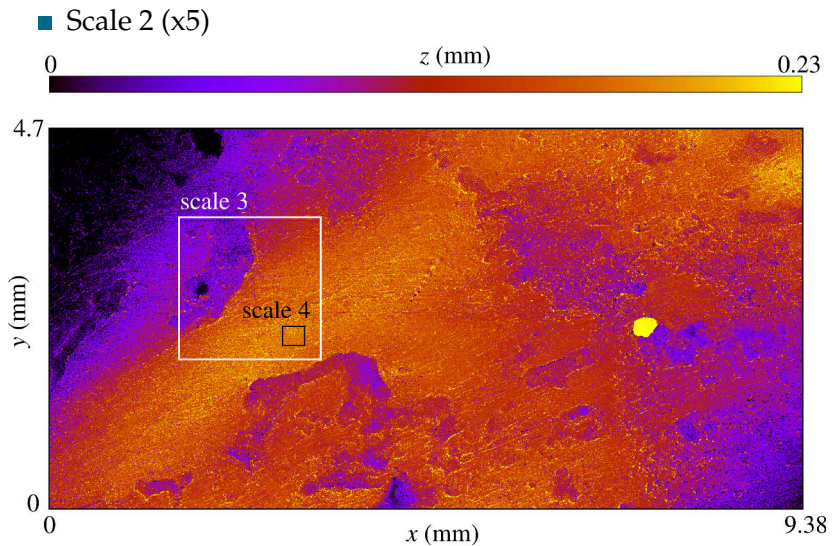
Multiscale road roughness



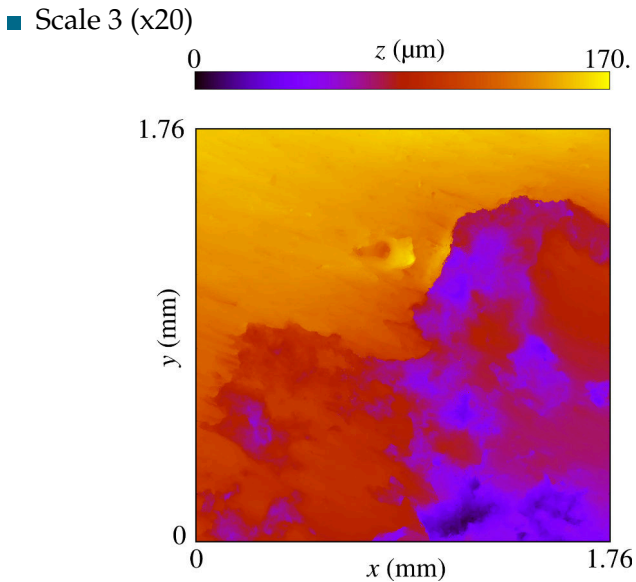
Multiscale road roughness



Multiscale road roughness

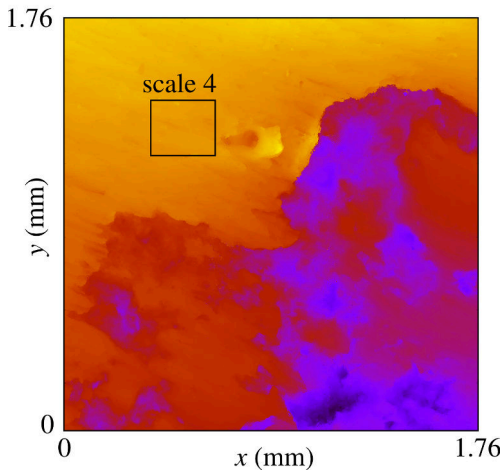


Multiscale road roughness



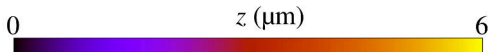
Multiscale road roughness

■ Scale 3 (x20)



Multiscale road roughness

■ Scale 4 (x100)



0.236

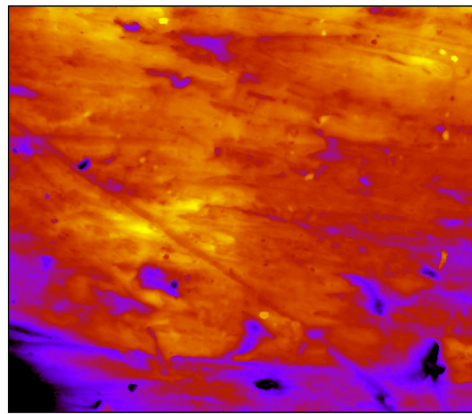
y (mm)

0

0

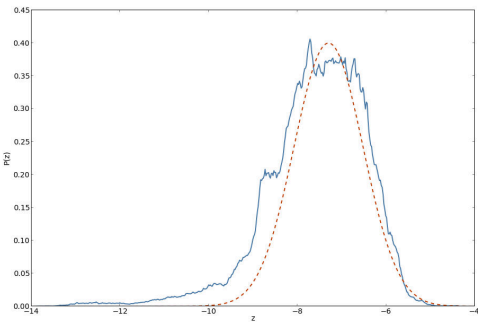
x (mm)

0.274



Multiscale road roughness

- Scale 4 (x100): PDF



What did you learn?

- Idea about the interface physics complexity
- How to measure roughness: confocal, WLI, AFM, STM
- What are the main characteristics: PDF, PSD, S_q , S_{dq} , Hurst, Nayak's parameter, etc
- Model roughness
- Fractal aspect & Mandelbrot set
- Real roughness



Thank you for your attention!
